

Exciton-cyclotron resonance in two-dimensional structures in a strong perpendicular magnetic field and optical orientation conditions

S. A. Moskalenko,^{1,*} M. A. Liberman,² and I. V. Podlesny¹

¹*Institute of Applied Physics, Academy of Sciences of Moldova, 5, Academiei str., MD-2028 Chisinau, Republic of Moldova*

²*Department of Physics, Uppsala University, P.O. Box 530, SE-751 21 Uppsala, Sweden*

(Received 30 July 2008; revised manuscript received 10 February 2009; published 23 March 2009)

The absorption band shapes of the combined optical quantum transitions with creation of the two-dimensional magnetoexcitons and simultaneous excitation of one background electron from its lowest to the first-excited Landau level by circularly polarized radiation under the conditions of optical orientation and spin polarization are investigated. The light absorption in the frame of dipole-active transition is described in the second-order perturbation theory taking into account as the perturbations the electron-photon interaction and the electron-electron Coulomb interaction. The Hamiltonian of the electron-photon interaction depends on the directions of the light propagation and its circular polarization relative to the magnetic field direction and the electron-heavy-hole alignment with regard to the plane of the layer. It is shown that the probability of the combined absorption rate is four times larger if the optically created electron has the same spin projection as the background electrons, compared to the case when the electrons have antiparallel spins. The probability of quantum transition and the absorption band peaks decrease with the increased magnetic field as $H^{-1/2}$ at a given filling factor ν^2 . If photocreated electron and hole have the same numbers of the Landau levels, $n_e = n_h$, the quantum transitions are dipole active. If these numbers differ by one, the quantum transition is quadrupole active, depends on the projections of the light wave vector on the plane of the layer, and vanishes in the Faraday geometry.

DOI: [10.1103/PhysRevB.79.125425](https://doi.org/10.1103/PhysRevB.79.125425)

PACS number(s): 71.35.Cc, 71.35.Ji, 73.21.Fg, 71.35.Gg

I. INTRODUCTION

The many-body combined quantum processes in the two-dimensional (2D) electron gas (2DEG) in a magnetic field, whose manifestation can be observed by characteristic features in optical spectra, attracted considerable attention during past years.^{1–20} A large variety of optically active excitations including magnetoplasmons in quantum well structures¹¹ was discussed. The fractionally charged quasiexcitons,^{12,15} dressed excitons,¹⁶ and anyon excitons¹⁷ can be formed if optically injected valence-band hole interacts with the surrounding electrons forming 2DEG in the regime of the fractional quantum Hall effect. Another aspect of the many-body interaction is the many-particle scattering, such as shake-up (SU) process in photoluminescence^{1–7} (PL) and a closely related to the SU processes—the combined exciton-cyclotron resonance (ExCR) in absorption spectra of 2DEG.^{8,9} All these processes take place when a supplementary e - h pair is optically created in the two-dimensional hole gas (2DHG). From experimental point of view, the system response to the optical probe can reveal fine correlations under these conditions. The recombination of the electron and hole accompanied by ejection of the second electron to higher Landau levels (LLs) gives rise to a fan of discrete lines SU_n with $n=1, 2, \dots$ associated with different Landau levels,^{4–6} which were observed in the PL spectra of high-density 2DEG.² The well-resolved new emission lines were observed in the range of phonon replicas¹ and the resonant interaction between LO-phonon and shake-up satellites was found in Ref. 4. The SU processes can also accompany the trion recombination⁴ and they form an important evidence for the three-body structure. The SU processes depend on the density of background electrons, reflecting the single-particle

nature of the excitation in the dilute limit. At high electron densities, the single-particle excitation transforms to creation of magnetoplasmons displaying a nontrivial dispersion.¹¹

The cyclotron replica AX^+SU corresponding to shake-up process with the participation of the acceptor-bound trion AX^+ was recently observed⁷ in 2DHG, where the magneto-optical probing of the weak disorder in 2DHG was studied with additional e - h pairs introduced into the system via photoabsorption. The observed low energy tail is plausibly due to inhomogeneous broadening related to different distances between the acceptor and the trion X^+ in a strong magnetic field.

In the present paper we consider theory of the combined ExCR in the low-density 2DEG system of a semiconductor quantum well. First, the ExCR has been studied experimentally and theoretically in Refs. 8 and 9 where the theory was developed for a weak magnetic field when the magnetic length is much larger than the exciton Bohr radius and the exciton Rydberg constant is greater than the distance between the LLs. Here an incident photon creates a Wannier-Mott exciton and simultaneously excites one of the resident electrons from the lowest to higher LLs. The PL spectra, the photoluminescence excitation (PLE) spectra, and reflectivity spectra were used to determine the ExCR line. The energy position of this line lies in the range of the Coulomb bound states representing the discrete energy spectrum of the relative e - h motion of 2D Wannier-Mott exciton. It was found that the ExCR line shifts linearly with the magnetic field strength with a slope comparable to the electron cyclotron frequency. While for higher illumination intensity, i.e., for larger $n_{el}(r)$, the exciton lines remain insensitive, the intensity of the ExCR line increases and the ExCR line is strongly σ^- polarized. Yakovlev and co-workers^{8,9} supposed that the

modifications of the Wannier-Mott exciton wave functions under the influence of magnetic field and background electron concentration are negligible. They found that the obtained probability of the quantum transitions decreases with the increase in the magnetic field. In the limit of a strong magnetic field, ExCR was considered in Refs. 13, 14, and 20 in the frame of more general theory of the charged e - h complexes.

In the present paper, we consider regime of strong magnetic fields when the distance between Landau levels is larger than the exciton Rydberg and the magnetic length is smaller than the exciton Bohr radius. Otherwise, we adopted the same assumptions as in Refs. 8 and 9 assuming the concentration of the resident electrons to be small and that they do not influence the structure of magnetoexcitons. In the case of a strong magnetic field, this phenomenon can be described in the frame of the first- and second-order perturbation theories taking into account as perturbations the electron-photon interaction as well as the Coulomb electron-electron interaction. The first-order approach uses the electron-photon interaction as a perturbation without addressing the Coulomb electron-electron interaction. In this case, the described process is a three-particle resonance involving two electrons and one hole when the incident photon creates an exciton from the hole and one background electron, whereas another optically excited electron is created directly on the excited Landau level. We developed a rigorous theory of the ExCR on the base of the dipole-active quantum transitions in the frame of the second-order perturbation theory using as perturbations the electron-photon interaction and the electron-electron Coulomb interaction. The developed theory also explains some features of recently observed⁷ luminescence spectra in the two-dimensional hole gas accompanied by the shake-up processes.

In a semiconductor quantum well structure of the type CdTe, the electrons belong to s -type conduction band with spin projections $s_z = \pm 1/2$, whereas the heavy holes are formed in p -type valence band with orbital momentum projection $M = \pm 1$. The heavy holes with the total momentum projections $j_z = \mp 3/2$ and electrons with spin projection $s_z = \pm 1/2$ form electron-hole pairs with $F = s_z + j_z = \mp 1$ coinciding with the orbital quantum number M . Without a magnetic field the band-to-band quantum transitions are allowed, whereas in the presence of a strong perpendicular magnetic field they are dipole active when the created e - h pair has the same Landau quantum numbers $n_e = n_h$, and they are quadrupole active when the quantum numbers differ by 1, i.e., $n_e = n_h \pm 1$. It will be shown that in the later case the probability of quantum transition is proportional to $|\vec{Q}_{2D}|^2$, where \vec{Q}_{2D} is the projection of the light wave vector \vec{Q} on the layer surface, which vanishes in the Faraday geometry of excitation.

The paper is organized as follows. In Sec. II the Hamiltonian of the electron-radiation interaction is obtained in the presence of a strong perpendicular magnetic field for the Faraday geometry when the light is propagating along the direction of the magnetic field and in the case of an arbitrary orientation of the light wave vectors and their circular polarizations with regard to the direction of magnetic field and of the magnetoexciton orbital momentum with projections M

$= \pm 1$ formed by its heavy-hole component. The background electrons can influence the form of the lowest magnetoexciton absorption band itself creating its pedestal without participating in the cyclotron quantum transitions. This can be described in the frame of the first-order perturbation theory taking into account the dipole-active optical transitions. The combined quantum transitions with the creation of a magnetoexciton with lowest quantum numbers of the Landau levels for the electron and hole and excitation of a background electron from the lowest to the first-excited Landau level are considered in the second order of the perturbation theory when the dipole-active optical quantum transitions are involved in combination with the Coulomb electron-electron interaction. The first step of the perturbation theory in the frame of this model is the incident photon creating an electron-hole pair. Optically created electron interacts with one background electron giving rise to one electron in the final magnetoexciton state and to another electron on the excited Landau level. In the Landau gauge the electron states are labeled by $(n;p)$, where n is the quantum number of the Landau quantization and p is one-dimensional (1D) wave vector. Two electrons taking part in the Coulomb scattering process have the initial quantum numbers $(0;f)$ and $(0;h)$, whereas their final quantum numbers are $(1;R)$ and $(0;T)$. The corresponding matrix element of the Coulomb electron-electron interaction denoted as $F_{e-e}(0,f;0,h;1,R;0,T)$ was studied in Refs. 21 and 22. In Sec. III the optical orientation, spin polarization, and alignment of 2D magnetoexcitons in the presence of background electrons are discussed. In Sec. IV the absorption band shapes of the combined quantum transitions are obtained in Faraday geometry for two circular light polarizations. We conclude with a discussion of how theoretical findings explain features of the optical spectra of ExCR and the photoluminescence spectra of the 2DHG observed recently in Ref. 7.

II. HAMILTONIAN OF THE ELECTRON-RADIATION INTERACTION

We shall start with derivation of the electron-radiation Hamiltonian in the second quantization representation for the case of a 2D electron-hole system in a strong magnetic field perpendicular to the surface of the semiconductor layer. We consider the light with circular polarization $\vec{\sigma}_{\vec{k}}$ around the photon wave vector \vec{k} arbitrary oriented in the three-dimensional (3D) space exciting the e - h pairs in the plane of the 2D layer. The s -type conduction-band electrons with spin projections along the magnetic field direction $s_z = \pm 1/2$ and the holes in the valence band with in-plane oriented p -type orbital wave functions and orbital momentum projections on the magnetic field direction $M = \pm 1$ are discussed. Only two of the six states of the heavy holes with total momentum projections $j_z = \pm 3/2$ will be taken into account. Together with the electrons they form two states $(e, s_z = +1/2; h, j_z = -3/2)$ and $(e, s_z = -1/2; h, j_z = +3/2)$ of the dipole-active bright exciton with $F = s_z + j_z = \mp 1$ correspondingly. For bright excitons the summary projection F coincides with the orbital quantum number M .

We shall consider only the band-to-band quantum transitions with the participation of the heavy holes. The electron-

radiation interaction in the linear approximation on the vector-potential $\vec{A}(\vec{r})$ in the coordinate representation is

$$H_{e\text{-rad}} = \left(-\frac{e}{m_0 c} \right) \sum_i \vec{A}(\vec{r}_i) \hat{P}_i, \quad (1)$$

where i numerates the electrons of the semiconductor. The vector potential $\vec{A}(\vec{r})$ of the electromagnetic field is determined as

$$\vec{A}(\vec{r}) = \sum_{\vec{k}} \sum_j \sqrt{\frac{2\pi\hbar c^2}{V\omega_Q}} \vec{e}_{\vec{k},j} (e^{i\vec{k}\vec{r}} C_{\vec{k},j} + e^{-i\vec{k}\vec{r}} C_{\vec{k},j}^\dagger). \quad (2)$$

Here $C_{\vec{k},j}^\dagger$ and $C_{\vec{k},j}$ are the photon creation and annihilation operators with 3D wave vector \vec{k} and with linear polarizations $\vec{e}_{\vec{k},1}$ and $\vec{e}_{\vec{k},2}$ obeying the transversality condition,

$$(\vec{e}_{\vec{k},j} \cdot \vec{k}) = 0, \quad j = 1, 2. \quad (3)$$

$\omega = ck$ is the photon frequency and V is the volume of the 3D space, where the light is propagating in the surroundings of the 2D layer with a surface area S . When the layer is embedded inside the microcavity and the electromagnetic field is confined between the mirrors of the resonator with the length L , then $V = SL$.

The single electron wave functions have the forms of the crystal Bloch functions and describe the electron in s -type conduction band with $s_z = \pm 1/2$ along the magnetic field direction, as well as the electron in the p -type valence band with spin-orbital coupling and quantum number $j = 3/2$ of the total momentum. Only its projections $j_z = \pm 3/2$ are involved. The selected electron Bloch functions are

$$\begin{aligned} \Psi_{c,s,1/2,\vec{q}} &= \frac{e^{i\vec{q}\vec{r}}}{\sqrt{V}} U_{c,s,\vec{q}}(\vec{r}) |\uparrow\rangle, \\ \Psi_{c,s,-1/2,\vec{q}} &= \frac{e^{i\vec{q}\vec{r}}}{\sqrt{V}} U_{c,s,\vec{q}}(\vec{r}) |\downarrow\rangle, \\ \Psi_{v,p,3/2,3/2,\vec{q}} &= \frac{e^{i\vec{q}\vec{r}}}{\sqrt{2V}} [U_{v,p,x,\vec{q}}(\vec{r}) + iU_{v,p,y,\vec{q}}(\vec{r})] |\uparrow\rangle, \\ \Psi_{v,p,3/2,-3/2,\vec{q}} &= \frac{e^{i\vec{q}\vec{r}}}{\sqrt{2V}} [U_{v,p,x,\vec{q}}(\vec{r}) - iU_{v,p,y,\vec{q}}(\vec{r})] |\downarrow\rangle. \end{aligned} \quad (4)$$

Here $U_{c,s,\vec{q}}(\vec{r})$, $U_{v,p,x,\vec{q}}(\vec{r})$, and $U_{v,p,y,\vec{q}}(\vec{r})$ are the periodic parts of the Bloch functions and the spin functions $|\uparrow\rangle$ and $|\downarrow\rangle$ describe the spin orientation along the magnetic field. The x and y axes are oriented in plane of the layer. In the bulk crystals the envelope functions $\frac{e^{i\vec{q}\vec{r}}}{\sqrt{V}}$ have the form of plane waves. Two coordinate wave functions of the types $(x \pm iy)$ have the orbital momentum projections on the magnetic field direction $M = \pm 1$ and can be characterized by two circular polarization vectors $\vec{\sigma}_M$,

$$\vec{\sigma}_M = \frac{1}{\sqrt{2}} (\vec{a}_1 \pm i\vec{a}_2), \quad M = \pm 1. \quad (5)$$

Here \vec{a}_1 and \vec{a}_2 are the unit vectors in the directions of the x and y axes. Side by side with circular polarization of the light we have introduced the notion of circular polarization vectors $\vec{\sigma}_M$ of valence electrons, heavy holes, and magnetoexcitons. The values of M , or of the vectors $\vec{\sigma}_M$, characterize supplementary the magnetoexciton states side by side with the numbers, n_e and n_h , of the Landau levels of electron and of hole correspondingly and with the 2D exciton wave vector \vec{k}_{ex} . The full set of quantum numbers is $(n_e, n_h, M, \vec{k}_{\text{ex}})$. The periodic parts of the Bloch wave functions remain the same in the case of 2D layer, as in the bulk crystals. The 2D layer has, in fact, a monoatomic width. The envelope functions in Landau gauge have the forms

$$\Psi_{n,q}(\vec{r}) = \frac{e^{iqx}}{\sqrt{L_x}} \varphi_n(x - ql_0^2). \quad (6)$$

Here L_x is the linear dimension of the layer, $l_0^2 = \frac{\hbar c}{eH}$ is the magnetic length, n is the number of the discrete level of Landau quantization in one in-plane direction, and q is the 1D wave vector of the plane wave describing the translational motion in another in-plane direction perpendicular to the previous one.

The wave functions of the conduction and valence electrons and the corresponding creation and annihilation operators are denoted as

$$a_{\pm 1/2, n_e, q}^\dagger, \quad a_{\pm 1/2, n_e, q}, \quad a_{\pm 3/2, n_v, q}^\dagger, \quad a_{\pm 3/2, n_v, q}. \quad (7)$$

The spin projections $s_z = \pm 1/2$ and Landau quantum number n_c describe the states of conduction electrons, whereas the projections of the total momentum $j_z = \pm 3/2$ and quantum number n_v concern the valence electrons.

Optical orientation effects are related with the absorption and emission of the circularly polarized light, with vectors of the circular polarizations,

$$\begin{aligned} \vec{\sigma}_k^\pm &= \frac{1}{\sqrt{2}} (\vec{e}_{\vec{k},1} \pm i\vec{e}_{\vec{k},2}), \\ (\vec{\sigma}_k^\pm)^* &= \frac{1}{\sqrt{2}} (\vec{e}_{\vec{k},1} \mp i\vec{e}_{\vec{k},2}). \end{aligned} \quad (8)$$

We introduce the photon creation and annihilation operators with the same quantum numbers,

$$\begin{aligned} C_{\vec{k},\pm} &= \frac{1}{\sqrt{2}} (C_{\vec{k},1} \pm iC_{\vec{k},2}), \\ (C_{\vec{k},\pm})^\dagger &= \frac{1}{\sqrt{2}} (C_{\vec{k},1}^\dagger \mp iC_{\vec{k},2}^\dagger). \end{aligned} \quad (9)$$

The relations between the operators in two different linear and circular polarizations are

$$\begin{aligned}
\sum_{j=1}^2 C_{\vec{k},j}^{\dagger} \vec{e}_{\vec{k},j} &= \vec{\sigma}_{\vec{k}}^{\dagger} C_{\vec{k},-}^{\dagger} + \vec{\sigma}_{\vec{k}}^{-} C_{\vec{k},+}^{\dagger} + \sum_{j=1}^2 C_{\vec{k},j}^{\dagger} \vec{e}_{\vec{k},j} \\
&= (\vec{\sigma}_{\vec{k}}^{\dagger})^* (C_{\vec{k},-}^{\dagger})^{\dagger} + (\vec{\sigma}_{\vec{k}}^{-})^* (C_{\vec{k},+}^{\dagger})^{\dagger} \\
&= \vec{\sigma}_{\vec{k}}^{-} \frac{1}{\sqrt{2}} (C_{\vec{k},1}^{\dagger} + i C_{\vec{k},2}^{\dagger}) + \vec{\sigma}_{\vec{k}}^{\dagger} \frac{1}{\sqrt{2}} (C_{\vec{k},1}^{\dagger} - i C_{\vec{k},2}^{\dagger}).
\end{aligned} \tag{10}$$

The circular polarization $\vec{\sigma}_{\vec{k}}^{\pm}$ has the orbital projections $M_{\vec{k}} = \pm 1$ on the direction of the wave vector \vec{k} correspondingly. The annihilation of the photon with quantum number (\vec{k}, \pm) means the loss of the orbital projection $M_{\vec{k}} = \mp 1$ in the same direction.

The Hamiltonian of the electron-radiation interaction in the second quantization representation describing only the band-to-band optical transitions using the electron creation and annihilation operators [Eq. (7)] is derived in Appendix A

and is represented by formula (A12). It will be transcribed below in the electron-hole creation and annihilation operators. We will take into account that the projections of heavy hole j_z and its wave vectors q have opposite signs to the corresponding values of the valence electron. Due to the negative value of the valence electron effective mass $m_v = -|m_v| = -m_h$ their energy spectrum of the Landau quantization is negative, which means that the hole's energy spectrum of Landau quantization is positive at the same numbers $n_v = n_h$. In the following the conduction electron will be named simply as electron writing $n_c = n_e$. The creation and annihilation operators are

$$a_{\pm 1/2, n_e, g} = a_{\pm 1/2, n_c, g}, \quad b_{\pm 3/2, n_h, q} = a_{\mp 3/2, n_v, -q}, \tag{11}$$

$$b_{\pm 3/2, n_h, q} = a_{\mp 3/2, n_v, -q}.$$

Being transcribed in these operators Hamiltonian (A12) takes the form

$$\begin{aligned}
\hat{H}_{e\text{-rad}} &= \left(-\frac{e}{m_0} \right) \sum_{\vec{k}(k_x, k_y, k_z)} \sqrt{\frac{2\pi\hbar}{V\omega_k}} \sum_{n_e, n_h} \sum_p \{ P_{cv}(k_y, p) \Phi(n_e, p; n_h, p - k_x; k_y) [(C_{\vec{k},-}^{\dagger} \vec{\sigma}_{\vec{k}}^{\dagger} \cdot \vec{\sigma}_1) + C_{\vec{k},+}^{\dagger} (\vec{\sigma}_{\vec{k}}^{-} \cdot \vec{\sigma}_1)] a_{1/2, n_e, p}^{\dagger} b_{-3/2, n_h, k_x - p}^{\dagger} \\
&+ [C_{\vec{k},-}^{\dagger} (\vec{\sigma}_{\vec{k}}^{\dagger} \cdot \vec{\sigma}_{-1}) + C_{\vec{k},+}^{\dagger} (\vec{\sigma}_{\vec{k}}^{-} \cdot \vec{\sigma}_{-1})] a_{1/2, n_e, p}^{\dagger} b_{3/2, n_h, k_x - p}^{\dagger} + P_{cv}^*(-k_y, p) \Phi^*(n_e, p; n_h, p + k_x; -k_y) [(C_{\vec{k},-}^{\dagger} (\vec{\sigma}_{\vec{k}}^{\dagger} \cdot \vec{\sigma}_{-1}) \\
&+ C_{\vec{k},+}^{\dagger} (\vec{\sigma}_{\vec{k}}^{-} \cdot \vec{\sigma}_{-1})] b_{-3/2, n_h, -p - k_x} a_{1/2, n_e, p} + [C_{\vec{k},-}^{\dagger} (\vec{\sigma}_{\vec{k}}^{\dagger} \cdot \vec{\sigma}_1) + C_{\vec{k},+}^{\dagger} (\vec{\sigma}_{\vec{k}}^{-} \cdot \vec{\sigma}_1)] b_{3/2, n_h, -p - k_x} a_{-1/2, n_e, p} + P_{cv}(-k_y, p) \Phi(n_e, p; n_h, p + k_x; \\
&- k_y) [(C_{\vec{k},+}^{\dagger} (\vec{\sigma}_{\vec{k}}^{\dagger} \cdot \vec{\sigma}_1) + (C_{\vec{k},-}^{\dagger} (\vec{\sigma}_{\vec{k}}^{-} \cdot \vec{\sigma}_1)] a_{1/2, n_e, p}^{\dagger} b_{-3/2, n_h, -p - k_x}^{\dagger} + [(C_{\vec{k},+}^{\dagger} (\vec{\sigma}_{\vec{k}}^{\dagger} \cdot \vec{\sigma}_{-1}) + (C_{\vec{k},-}^{\dagger} (\vec{\sigma}_{\vec{k}}^{-} \cdot \vec{\sigma}_{-1})] a_{-1/2, n_e, p}^{\dagger} b_{3/2, n_h, -p - k_x}^{\dagger} \\
&+ P_{cv}^*(k_y, p) \Phi^*(n_e, p; n_h, p - k_x; k_y) [(C_{\vec{k},+}^{\dagger} (\vec{\sigma}_{\vec{k}}^{\dagger} \cdot \vec{\sigma}_{-1}) + (C_{\vec{k},-}^{\dagger} (\vec{\sigma}_{\vec{k}}^{-} \cdot \vec{\sigma}_{-1})] b_{-3/2, n_h, k_x - p} a_{1/2, n_e, p} \\
&+ [(C_{\vec{k},+}^{\dagger} (\vec{\sigma}_{\vec{k}}^{\dagger} \cdot \vec{\sigma}_1) + (C_{\vec{k},-}^{\dagger} (\vec{\sigma}_{\vec{k}}^{-} \cdot \vec{\sigma}_1)] b_{3/2, n_h, k_x - p} a_{-1/2, n_e, p} \}. \tag{12}
\end{aligned}$$

If one is interested only in the resonant part of Hamiltonian (12), it has the form

$$\begin{aligned}
\hat{H}_{e\text{-rad}} &= \left(-\frac{e}{m_0} \right) \sum_{\vec{k}(k_x, k_y, k_z)} \sqrt{\frac{2\pi\hbar}{V\omega_k}} \sum_{n_e, n_h} \sum_p \{ P_{cv}(k_y, p) \Phi(n_e, p; n_h, p - k_x; k_y) [(C_{\vec{k},-}^{\dagger} (\vec{\sigma}_{\vec{k}}^{\dagger} \cdot \vec{\sigma}_1) + C_{\vec{k},+}^{\dagger} (\vec{\sigma}_{\vec{k}}^{-} \cdot \vec{\sigma}_1)] a_{1/2, n_e, p}^{\dagger} b_{-3/2, n_h, k_x - p}^{\dagger} \\
&+ [C_{\vec{k},-}^{\dagger} (\vec{\sigma}_{\vec{k}}^{\dagger} \cdot \vec{\sigma}_{-1}) + C_{\vec{k},+}^{\dagger} (\vec{\sigma}_{\vec{k}}^{-} \cdot \vec{\sigma}_{-1})] a_{1/2, n_e, p}^{\dagger} b_{3/2, n_h, k_x - p}^{\dagger} + P_{cv}^*(k_y, p) \Phi^*(n_e, p; n_h, p - k_x; k_y) [(C_{\vec{k},+}^{\dagger} (\vec{\sigma}_{\vec{k}}^{\dagger} \cdot \vec{\sigma}_{-1}) \\
&+ (C_{\vec{k},-}^{\dagger} (\vec{\sigma}_{\vec{k}}^{-} \cdot \vec{\sigma}_{-1})] b_{-3/2, n_h, k_x - p} a_{1/2, n_e, p} + [(C_{\vec{k},+}^{\dagger} (\vec{\sigma}_{\vec{k}}^{\dagger} \cdot \vec{\sigma}_1) + (C_{\vec{k},-}^{\dagger} (\vec{\sigma}_{\vec{k}}^{-} \cdot \vec{\sigma}_1)] b_{3/2, n_h, k_x - p} a_{-1/2, n_e, p} \}. \tag{13}
\end{aligned}$$

In the case of Faraday geometry, when the light wave vector \vec{k} is parallel to the direction of magnetic field, when the quadrupole-active quantum transition vanish and the supplementary requirement $n_e = n_h$ holds, we can put $\vec{\sigma}_{\vec{k}}^{\pm} = \vec{\sigma}_{\pm 1}$. In this special case Hamiltonian (13) becomes

$$\begin{aligned}
\hat{H}_{e\text{-rad}} &= \left(-\frac{e}{m_0} \right) \sum_{\vec{k}(k_x, k_y, k_z)} \sqrt{\frac{2\pi\hbar}{V\omega_k}} \sum_n \sum_p \{ P_{cv}(0, p) [C_{\vec{k},+}^{\dagger} a_{1/2, n, p}^{\dagger} b_{-3/2, n, -p}^{\dagger} + C_{\vec{k},-}^{\dagger} a_{-1/2, n, p}^{\dagger} b_{3/2, n, -p}^{\dagger}] + P_{cv}^*(0, p) [(C_{\vec{k},+}^{\dagger})^{\dagger} b_{-3/2, n, -p} a_{1/2, n, p} \\
&+ (C_{\vec{k},-}^{\dagger})^{\dagger} b_{3/2, n, -p} a_{-1/2, n, p} \}]. \tag{14}
\end{aligned}$$

Hamiltonians (12)–(14) and (A12) demonstrate dependences of the amplitudes of quantum transitions as well as of their probabilities on the reciprocal orientations of the pho-

ton circular polarization vectors $\vec{\sigma}_{\vec{k}}^{\pm}$ with regard to the circular polarization vectors $\vec{\sigma}_M$ describing the heavy-hole orbital structure. $\vec{\sigma}_M$ becomes a supplementary characteristic of e - h

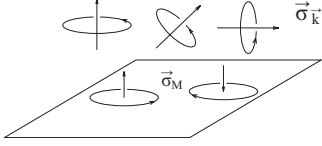


FIG. 1. The reciprocal orientations of the circularly polarized vectors $\vec{\sigma}_k^\pm$ and $\vec{\sigma}_M$.

pair as a whole as well as of the magnetoexciton. Different orientations of $\vec{\sigma}_k^\pm$ relative to the layer are illustrated in Fig. 1. Their contributions to the probabilities of the quantum transitions are expressed by the factors

$$f = |(\vec{\sigma}_k^\pm \cdot \vec{\sigma}_M)|^2. \quad (15)$$

As was mentioned above in the Faraday geometry when \vec{k} is parallel to the magnetic field direction we have $\vec{\sigma}_k^\pm = \vec{\sigma}_{\pm 1}$. For the case of the Voigt geometry the light wave vector \vec{k} lies in the plane of the layer and its circular polarization vectors are, for example, $\vec{\sigma}_{a_1}^\pm = \frac{1}{\sqrt{2}}(\vec{a}_2 \pm i\vec{a}_3)$, where \vec{a}_3 is the unit vector in the direction perpendicular to the layer surface. The scalar product of $\vec{\sigma}_{a_1}^\pm$ with the circular polarization vectors $\vec{\sigma}_M = \frac{1}{\sqrt{2}}(\vec{a}_1 \pm i\vec{a}_2)$ gives the probability factor $|(\vec{\sigma}_{a_1}^\pm \cdot \vec{\sigma}_M)|^2 = \frac{1}{4}$ for four different combinations.

Another property of Hamiltonian (14) with axial symmetry in the Faraday geometry is the conservation law for the orbital momentum projections. For example, photons described by the annihilation operators $C_{\vec{k}, \pm}$ are accompanied by the circular polarization vectors $\vec{\sigma}_k^\mp$ with the orbital momentum projections $M = \mp 1$ correspondingly. After annihilation of these photons the electron-hole pairs with the same values of M will appear and vice versa.

This conservation law holds also in the case of antiresonant terms of the Hamiltonian with axial symmetry. The antiresonant terms describe simultaneous creation and annihilation of one photon and of one e - h pair with opposite sign orbital momentum projections so that their summary projection equals zero. The conservation law does not hold if the axial symmetry of the system is broken due to arbitrary direction of the light propagation.

The exciton creation operators in Landau gauge can be constructed following Refs. 21 and 22,

$$\Psi_{\text{ex}}^{(n,m)\dagger}(\vec{k}, M = \pm 1) = \frac{1}{\sqrt{N}} \sum_t e^{ik_y t} a_{\mp 1/2, n, k_x/2+t}^\dagger b_{\pm 3/2, m, k_x/2-t}^\dagger. \quad (16)$$

They are characterized by the quantum numbers n and m of Landau quantization levels for electron and for hole correspondingly by the 2D wave vector \vec{k} with projections k_x and k_y and by the combinations of the electron-spin projections $s_z = \pm 1/2$ and by the heavy-hole full momentum projection $j_z = \mp 3/2$, so that to form the resultant projections $F = s_z + j_z = M = \mp 1$. The creation energy of the magnetoexciton levels without Zeeman splitting is

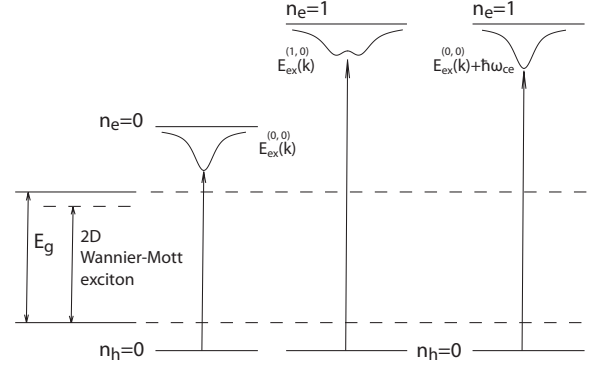


FIG. 2. The scheme of two magnetoexciton energy bands $E_{\text{ex}}^{(0,0)}(k)$ and $E_{\text{ex}}^{(1,0)}(k)$ as well as of the combined magnetoexciton-cyclotron-resonance energy band, $E_{\text{ex}}^{(0,0)}(k) + \hbar\omega_{ce}$.

$$E_{\text{ex}}^{(n,m)}(\vec{k}, s_z, j_z) = E_g + \frac{1}{2}\hbar\omega_{c\mu} + n\hbar\omega_{ce} + m\hbar\omega_{ch} - I_{\text{ex}}^{(n,m)}(\vec{k}). \quad (17)$$

Here ω_{ce} , ω_{ch} , and $\omega_{c\mu}$ are the cyclotron frequencies calculated for the electron, hole, and reduced exciton masses, m_e , m_h , and $\mu = \frac{m_e m_h}{m_e + m_h}$, correspondingly. The ionization potentials of magnetoexcitons $I_{\text{ex}}^{(n,m)}(k)$ essentially depend on the electron and hole Landau quantum numbers n and m .^{21,22} The scheme of two magnetoexciton bands with quantum numbers $n_e = n_h = 0$ and $n_e = 1, n_h = 0$ is depicted in Fig. 2.

For the purposes of the present work we will need the Hamiltonian of the electron-electron Coulomb interaction, which has been derived in the papers^{21,22} and has the form

$$H_C = \frac{1}{2} \sum_{p', q', s'} \sum_{n', m'} \sum_{\sigma_1, \sigma_2} F_{e-e}(0, p'; 0, q'; n', p' - s'; m', q' + s') \times a_{\sigma_1, 0, p'}^\dagger a_{\sigma_2, 0, q'}^\dagger a_{\sigma_2, m', q' + s'} a_{\sigma_1, n', p' - s'} + \text{H.c.} \quad (18)$$

Here only the Coulomb scattering of two electrons with quantum transitions from the lowest Landau levels to two excited Landau levels n', m' was taken into account. The matrix elements of Coulomb interaction $F_{e-e}(0, p'; 0, q'; n', p' - s'; m', q' + s')$ were calculated in Refs. 21 and 22.

III. OPTICAL ORIENTATION, SPIN POLARIZATION, AND ALIGNMENT OF 2D MAGNETOEXCITONS IN THE PRESENCE OF BACKGROUND ELECTRONS

We shall consider the combined optical transitions with creation of one magnetoexciton and simultaneous excitation of one background electron from the lowest to the first-excited Landau level. We suppose that in the initial state there is a photon with wave vector \vec{Q} and circular polarization $\vec{\sigma}_Q^\mp$ on the direction of the wave vector, whereas the background electrons have the spin polarization $s_z = 1/2$ along the magnetic field and are situated on the lowest Landau level with $n_e = 0$. In the Landau gauge description their states are characterized in addition by the dimensional wave

vector T . One of them takes part in the initial state written in the form

$$|i, \mp; \uparrow, 0, T\rangle = (C_{\tilde{Q}_{\pm}})^{\dagger} a_{1/2,0,T}^{\dagger} |0\rangle, \quad (19)$$

where $(C_{\tilde{Q}_{\pm}})^{\dagger}$ and $a_{1/2,0,T}^{\dagger}$ are the photon and electron creation operators and the photon creation operator carries the circular polarization $\vec{\sigma}_{\tilde{Q}_{\pm}}^{\pm}$.

In the final state the magnetoexciton is characterized by the quantum numbers of Landau levels, by the 2D wave vector \vec{k}_{ex} , and by the orbital states of the heavy holes with projections $M = \pm 1$ on the direction of the external magnetic field. These states can be characterized by the circular polarization vector $\vec{\sigma}_M$. In our concrete case we will suppose $n_e = n_h = 0$. The final state $|F\rangle$ is represented by lowest magnetoexciton band and by the background electron on the first Landau level $n_e = 1$ with one-dimensional wave vector R as follows:

$$|F, \vec{k}_{\text{ex}}, \pm; \uparrow, 1, R\rangle = \hat{\Psi}_{\text{ex}}^{(0,0)\dagger}(\vec{k}_{\text{ex}}, \pm) a_{1/2,1,R}^{\dagger} |0\rangle. \quad (20)$$

Creation of an electron-hole pair with definite values of s_z and j_z by the circularly polarized light means the spin orientation, whereas the creation of magnetoexcitons with definite values of M means the optical alignment of the excitons. These effects can be achieved only using the circularly polarized radiation and all of them are known as optical orientation phenomena.²³

We will consider below different geometries of excitation including the Faraday geometry when the light propagation direction coincides with the direction of the magnetic field as well as the Voigt geometry when the light wave vector is oriented in plane of the layer. For the Faraday geometry the axial symmetry of the system is conserved and the light with a given circular polarization creates magnetoexcitons with the same circular polarization. The conservation law for the circular polarization, i.e., for the angular-momentum projection on the magnetic field direction, holds. In Voigt geometry of excitation the light with any circular polarization creates magnetoexcitons with both circular polarizations with the same probability. The combined quantum transitions with the creation of a magnetoexciton with $n_e = n_h$ and with the simultaneous excitation of a background electron can be described in dipole approximation only in the second order of the perturbation theory. When $n_e = n_h \pm 1$ this process can be described in the first-order perturbation theory taking into account the quadrupole quantum transitions, whose amplitudes are proportional to $(Q_x + iQ_y)l_0$ and their probabilities are proportional to $|\vec{Q}_{2D}|^2 l_0^2$, where \vec{Q}_{2D} is a 2D vector. In the Faraday geometry the wave vector \vec{Q}_{2D} equals zero and the probability of quantum transition vanishes.

The intermediate states $|u\rangle$ in the second-order perturbation theory involve the heavy holes and are also characterized by the quantum number M and by the hole circular polarization along the magnetic field direction. They are

$$|u, \mp, \uparrow\rangle = |u, \mp, f, g; \uparrow, 0, h\rangle = a_{\pm 1/2,0,f}^{\dagger} b_{\mp 3/2,0,g}^{\dagger} a_{1/2,0,h}^{\dagger} |0\rangle. \quad (21)$$

Below, for simplicity, we will neglect the Zeeman splittings of the electron, hole, and exciton levels.

The energies of the initial, final, and intermediate states without Zeeman splittings are

$$E_{i,\uparrow} = \hbar\omega_Q + E_g + \frac{1}{2}\hbar\omega_{ce},$$

$$E_{u,\pm,\uparrow} = 2E_g + \frac{1}{2}\hbar\omega_{c\mu} + \frac{1}{2}\hbar\omega_{ce},$$

$$E_{F,\pm,\uparrow} = 2E_g + \frac{1}{2}\hbar\omega_{c\mu} + \frac{3}{2}\hbar\omega_{ce} - I_{\text{ex}}^{(0,0)}(\vec{k}_{\text{ex}}),$$

$$E_{i,\uparrow} - E_{u,\pm,\uparrow} = \hbar\omega_Q - E_g - \frac{1}{2}\hbar\omega_{c\mu},$$

$$\begin{aligned} E_{i,\uparrow} - E_{F,\pm,\uparrow} &= \hbar\omega_Q - E_g - \frac{1}{2}\hbar\omega_{c\mu} - \hbar\omega_{ce} + I_{\text{ex}}^{(0,0)}(\vec{k}_{\text{ex}}) \\ &= \Delta + I_{\text{ex}}^{(0,0)}(\vec{k}_{\text{ex}}). \end{aligned} \quad (22)$$

Here we introduce the energy detuning Δ ,

$$\Delta = \hbar\omega_Q - E_g - \frac{1}{2}\hbar\omega_{c\mu} - \hbar\omega_{ce},$$

$$\omega_{c,e} = \frac{eH}{m_e c}, \quad \omega_{c,h} = \frac{eH}{m_h c}, \quad \omega_{c,\mu} = \omega_{c,e} + \omega_{c,h}. \quad (23)$$

The matrix elements of the electron-radiation interaction Hamiltonian $H_{e\text{-rad}}$ between the initial and the intermediate states are

$$\begin{aligned} \langle i, \mp, \uparrow, 0, T | \hat{H}_{e\text{-rad}} | u, -, f, g; \uparrow, 0, h \rangle &= A(Q_y, Q_x - g) (\vec{\sigma}_{\tilde{Q}}^{\pm} \cdot \vec{\sigma}_{-1}) \\ &\times [\delta_{kr}(f, Q_x - g) \delta_{kr}(T, h) - \delta_{kr}(h, Q_x - g) \delta_{kr}(T, f)], \\ \langle i, \mp, \uparrow, 0, T | \hat{H}_{e\text{-rad}} | u, +, f, g; \uparrow, 0, h \rangle &= A(Q_y, Q_x - g) \\ &\times (\vec{\sigma}_{\tilde{Q}}^{\pm} \cdot \vec{\sigma}_1) \delta_{kr}(f, Q_x - g) \delta_{kr}(T, h), \end{aligned} \quad (24)$$

where

$$\begin{aligned} A(Q_y, Q_x - g) &= \left(-\frac{e}{m_0} \right) \sqrt{\frac{2\pi\hbar}{V\omega_Q}} \\ &\times P_{cv}^*(Q_y, Q_x - g) \Phi^*(0, Q_x - g; 0, -g; Q_y). \end{aligned} \quad (25)$$

Two matrix elements [Eq. (24)] differ from each other because the intermediate state $|u, -, \uparrow\rangle$ does contain two electrons with the same spin direction $s_z = 1/2$ and they both, being equivalent, take part interdependently in the optical quantum transitions. By this reason first matrix element (24) contains a direct and exchange terms. In the frame of the intermediate state $|u, +, \uparrow\rangle$ the two electrons have different

spins and they take part separately in the quantum transition. This difference essentially influences the combined quantum transition probability. The second step of the second-order perturbation theory is constructed on the base of Coulomb electron-electron interaction. In the frame of this step two electrons of the intermediate state being on the lowest Landau levels $n_{e1}=n_{e2}=0$ will be transformed into two another electrons, one in the composition of magnetoexciton with $n_e=n_h=0$ and another electron on the first-excited Landau level with $n_e=1$. Participation of both electrons with different spin orientations in Coulomb scattering processes is, of course, different due to the direct and exchange Coulomb interactions. In the second step of the perturbation theory the matrix elements of the Coulomb $e-e$ interaction do not vanish only between the intermediate and final states with the same quantum number M because the light is not involved and the symmetry of the 2D layer is conserved in the absence of the light influence. The matrix elements of the Coulomb interaction between the intermediate and the final states are

$$\begin{aligned} \langle u, -, \uparrow | \hat{H}_C | F, -, \uparrow \rangle &= \langle u, -, f, g; \uparrow, 0, h | \hat{H}_C | F, -, \vec{k}_{\text{ex}}, \uparrow, 1, R \rangle \\ &= \frac{\delta_{kr}(f+g+h-R, k_x)}{\sqrt{N}} e^{ik_y(k_x/2-g)t_0^2} \\ &\quad \times [F_{e-e}(0, h; 0, f; 1, R; 0, k_x - g) \\ &\quad - F_{e-e}(0, f; 0, h; 1, R; 0, k_x - g)], \\ \langle u, +, \uparrow | \hat{H}_C | F, +, \uparrow \rangle &= \langle u, +, f, g; \uparrow, 0, h | \hat{H}_C | F, +, \vec{k}_{\text{ex}}, \uparrow, 1, R \rangle \\ &= \frac{\delta_{kr}(f+g+h-R, k_x)}{\sqrt{N}} e^{ik_y(k_x/2-g)t_0^2} \\ &\quad \times F_{e-e}(0, f; 0, h; 0, k_x - g; 1, R), \\ \langle u, +, \uparrow | \hat{H}_C | F, -, \uparrow \rangle &= \langle u, -, \uparrow | \hat{H}_C | F, +, \uparrow \rangle = 0. \end{aligned} \quad (26)$$

The formulas [Eq. (26)] demonstrate the important role played by the background electron, which together with the optically new created electron takes part in the Coulomb scattering process giving rise to direct and exchange interaction terms in dependence on the spin directions of both electrons.

The conservation laws for the x components of the photon, magnetoexciton, and background electron momenta, which can be observed above, reflect the symmetry properties of 2D $e-h$ system in a strong perpendicular magnetic field revealed in Refs. 13, 20, and 24. Side by side with the canonical momentum operator \hat{P} and kinematic momentum operator $\hat{\pi}$, the magnetic momentum operator \hat{K} was introduced. Its square value \hat{K}^2 does commute with the Hamiltonian, whereas its components \hat{K}_x and \hat{K}_y do commute each other when the $e-h$ complexes are neutral such as excitons and biexcitons and do not commute in the case of charged $e-h$ complexes as in the case of combined quantum transition. By this reason the momentum conservation law for magnetoexciton-photon quantum transition is characterized by the equality $\vec{k}_{\text{ex}} = \vec{Q}_{2D}$ for the 2D wave vectors, whereas

the combined quantum transition is governed by the conservation law only for one component of the involved momenta.

For the opposite spin polarization of the background electrons $s_z = -1/2$ there are new initial states $|i, \pm; \downarrow, 0, T\rangle$, intermediate states $|u, \pm, f, g; \downarrow, 0, h\rangle$, and final states $|F, \vec{k}_{\text{ex}}, \pm; \downarrow, 1, R\rangle$, and the matrix elements of the electron-radiation interaction are

$$\begin{aligned} \langle i, \mp; \downarrow, 0, T | \hat{H}_{e\text{-rad}} | u, +, f, g; \downarrow, 0, h \rangle &= (\vec{\sigma}_Q^\pm \cdot \vec{\sigma}_1) A(Q_y, Q_x - g) \\ &\quad \times [\delta_{kr}(f, Q_x - g) \delta_{kr}(h, T) - \delta_{kr}(h, Q_x - g) \delta_{kr}(f, T)], \\ \langle i, \mp; \downarrow, 0, T | \hat{H}_{e\text{-rad}} | u, -, f, g; \downarrow, 0, h \rangle &= (\vec{\sigma}_Q^\pm \cdot \vec{\sigma}_{-1}) A(Q_y, Q_x \\ &\quad - g) \delta_{kr}(f, Q_x - g) \delta_{kr}(h, T). \end{aligned} \quad (27)$$

Notice that these matrix elements differ from expressions [Eq. (24)] by different polarizations $\vec{\sigma}_{-1}$ and $\vec{\sigma}_1$. The matrix elements of the electron-electron Coulomb interaction between the intermediate and the final states depend essentially on the mutual spin orientation of the optically created electrons and the background electrons. They are parallel in the case $\langle u, -, \uparrow | H_C | F, -, \uparrow \rangle$ as well as in the case $\langle u, +, \downarrow | H_C | F, +, \downarrow \rangle$, while both are oriented in different directions of the magnetic field. In the same manner the matrix element $\langle u, -, \downarrow | H_C | F, -, \downarrow \rangle$ coincides with the matrix element $\langle u, +, \uparrow | H_C | F, +, \uparrow \rangle$ because in both cases the optically created electron has spin projection opposite to the background electron and the result is determined by the second expression in Eq. (26).

First-order matrix elements (24) and (26) are used to calculate the second-order matrix elements $Z(i|F)$ using a general formula,

$$Z(i|F) = \sum_u \frac{\langle i | H_{er} | u \rangle \langle u | H_C | F \rangle}{E_i - E_u}. \quad (28)$$

They are calculated in Appendix B.

The probabilities of the quantum transitions are calculated using the Fermi's golden rule,

$$P(\omega_Q; i; F) = \frac{2\pi}{\hbar} |Z(i|F)|^2 \delta(E_i - E_F), \quad (29)$$

which after summation over the final states $|F\rangle$ it can be expressed through the imaginary part of the response function $S(\omega_Q, i)$ as follows:

$$\sum_{|F\rangle} P(\omega_Q; i; F) = -\frac{2}{\hbar} \text{Im} S(\omega_Q, i),$$

where

$$\begin{aligned} S(\omega_Q, i) &= \langle i | \hat{H}_{er} \frac{1}{E_i - H_0 + i\delta} \hat{H}_C \\ &\quad \times \frac{1}{E_i - H_0 + i\delta} \hat{H}_C \frac{1}{E_i - H_0 + i\delta} \hat{H}_{er} | i \rangle \end{aligned} \quad (30)$$

and \hat{H}_0 is the zero-order Hamiltonian of the 2D electron-hole system in a strong perpendicular magnetic field.

To calculate the partial probabilities of the combined quantum transitions we will need expressions (B3), (B4), (B12), and (B13). On their base one can write

$$\begin{aligned} \frac{2\pi}{\hbar} |Z(+, \vec{k}_{\text{ex}} - \vec{Q}_{2D}, \uparrow, T, R)|^2 &= \delta_{kr}(Q_x + T, k_x + R) \\ &\times \frac{(2\pi)^2 B(\omega_Q)}{VN} |H(\vec{k}_{\text{ex}} - \vec{Q}_{2D})|^2, \\ \frac{2\pi}{\hbar} |Z(-, \vec{k}_{\text{ex}} - \vec{Q}_{2D}, \uparrow, T, R)|^2 &= \delta_{kr}(Q_x + T, k_x + R) \\ &\times 4 \frac{(2\pi)^2 B(\omega_Q)}{VN} |H(\vec{k}_{\text{ex}} - \vec{Q}_{2D}) \\ &- F(\vec{k}_{\text{ex}} - \vec{Q}_{2D})|^2, \end{aligned} \quad (31)$$

where

$$B(\omega_Q) = \frac{\left(\frac{e}{m_0}\right)^2 |P_{cv}|^2}{\omega_Q \left[\hbar \omega_Q - E_g - \frac{1}{2} \hbar \omega_{c\mu} \right]^2}. \quad (32)$$

The probability of combined quantum transition with participation of two electrons with parallel spins is proportional to the coefficient $|Z(-, \vec{k}_{\text{ex}} - \vec{Q}_{2D}, \uparrow, T, R)|^2$. It contains a supplementary factor 4 as compared with the probability expressed by the coefficient $|Z(+, \vec{k}_{\text{ex}} - \vec{Q}_{2D}, \uparrow, T, R)|^2$ describing participation of two electrons with antiparallel spin projections. Only the excitons states with $M=-1$ and with combination of the electron-spin projection $s_z=+1/2$ and of heavy-hole momentum projection $j_z=-3/2$ can supply an optically created electron with the same spin projection as of the background electrons. In the case when the background electrons have the spin $-1/2$, the magnetoexcitons with $M=+1$, i.e., $s_z=-1/2$ and $j_z=3/2$, will be able to strongly favor the combined quantum transition. If the light with its circular polarization can excite the magnetoexciton with $M=-1$ in the presence of background electrons with spin projection $s_z=1/2$ the probability of combined quantum transition will strongly increase. If the light is able to excite the magnetoexciton with $M=+1$ in the presence of background electrons with spin projection $s_z=-1/2$, the effect will be strong as in the previous case. In both cases the exchange Coulomb term $F(\vec{k}_{\text{ex}} - \vec{Q}_{2D})$ is present side by side with the direct Coulomb term $H(\vec{k}_{\text{ex}} - \vec{Q}_{2D})$. As we will see in Sec. IV the absorption band shapes in two cases [Eq. (31)] will also be different.

For four different combinations of light circular polarization and electron-spin polarization, formula (29) gives the following expressions for the probabilities:

$$\begin{aligned} P(\omega_Q; i, \mp, \uparrow; F, -, \uparrow) &= 4 |(\vec{\sigma}_Q^\pm \cdot \vec{\sigma}_{-1})|^2 \delta_{kr}(Q_x + T, k_x + R) \\ &\times \frac{(2\pi)^2 B(\omega_Q)}{NV} |H(\vec{k}_{\text{ex}} - \vec{Q}_{2D}) \\ &- F(\vec{k}_{\text{ex}} - \vec{Q}_{2D})|^2 \delta_{kr}[\Delta + I_{\text{ex}}^{(0,0)}(\vec{k})], \end{aligned}$$

$$\begin{aligned} P(\omega_Q; i, \mp, \uparrow; F, +, \uparrow) &= |(\vec{\sigma}_Q^\pm \cdot \vec{\sigma}_1)|^2 \delta_{kr}(Q_x + T, k_x + R) \\ &\times \frac{(2\pi)^2 B(\omega_Q)}{NV} |H(\vec{k}_{\text{ex}} - \vec{Q}_{2D})|^2 \delta_{kr} \\ &\times [\Delta + I_{\text{ex}}^{(0,0)}(\vec{k})]. \end{aligned} \quad (33)$$

Expressions in Eq. (33) are proportional to $1/N$ because we took into account the participation in the quantum transition of only one electron in the state $|1/2, 0, T\rangle$. In reality their full number N_e is equal to Nv^2 , where v^2 is the filling factor and their concentration is $n_{\text{el}} = v^2/2\pi l_0^2$. It means that the obtained probability must be summarized over T and multiplied by v^2 . The expressions [Eq. (33)] must be summarized also on the quantum numbers \vec{k}_{ex} and R of the final states taking into account that

$$\sum_{\vec{k}_{\text{ex}}} = \frac{S}{(2\pi)^2} \int d^2\vec{k}, \quad V = SL, \quad (34)$$

where L determines the dimension of the 3D space in the direction perpendicular to the layer surface. After these summations we will find the full probabilities,

$$W = \frac{v^2 S}{(2\pi)^2} \sum_T \sum_R \int d^2\vec{k} P(\omega_Q; i; F). \quad (35)$$

In the case of background electrons polarized in the direction of the magnetic field, the probabilities are

$$\begin{aligned} W(\omega_Q; \mp; -; \uparrow) &= 4 |(\vec{\sigma}_Q^\pm \cdot \vec{\sigma}_{-1})|^2 \frac{v^2 B(\omega_Q)}{L} \\ &\times \int d^2\vec{k} |H(\vec{k} - \vec{Q}_{2D}) - F(\vec{k} - \vec{Q}_{2D})|^2 \\ &\times \delta_{kr}[\Delta + I_{\text{ex}}^{(0,0)}(\vec{k})], \\ W(\omega_Q; \mp; +; \uparrow) &= |(\vec{\sigma}_Q^\pm \cdot \vec{\sigma}_1)|^2 \frac{v^2 B(\omega_Q)}{L} \\ &\times \int d^2\vec{k} |H(\vec{k} - \vec{Q}_{2D})|^2 \delta_{kr}[\Delta + I_{\text{ex}}^{(0,0)}(\vec{k})]. \end{aligned} \quad (36)$$

Thus for the case of background electrons polarized in the direction opposite to the magnetic field, we find for the full probabilities,

$$\begin{aligned} W(\omega_Q; \mp; +; \downarrow) &= 4 |(\vec{\sigma}_Q^\pm \cdot \vec{\sigma}_1)|^2 \frac{v^2 B(\omega_Q)}{L} \\ &\times \int d^2\vec{k} |H(\vec{k} - \vec{Q}_{2D}) - F(\vec{k} - \vec{Q}_{2D})|^2 \\ &\times \delta_{kr}[\Delta + I_{\text{ex}}^{(0,0)}(\vec{k})], \end{aligned}$$

$$W(\omega_Q; \mp; -; \downarrow) = |(\vec{\sigma}_{\vec{Q}}^{\pm} \cdot \vec{\sigma}_{-1})|^2 \frac{v^2 B(\omega_Q)}{L} \times \int d^2 \vec{k} |H(\vec{k} - \vec{Q}_{2D})|^2 \delta_{kr}(\Delta + I_{\text{ex}}^{(0,0)}(\vec{k})). \quad (37)$$

Probabilities (36) and (37) depend on the values $H(\vec{k} - \vec{Q}_{2D})$ and $F(\vec{k} - \vec{Q}_{2D})$, which were calculated in Appendix B.

IV. ABSORPTION BAND SHAPES IN FARADAY GEOMETRY AND TWO LIGHT CIRCULAR POLARIZATIONS

The obtained expressions (36), (37), and (B14) depend essentially on the orientation of the light wave vector projection \vec{Q}_{2D} on the plane of the layer. The simplest case corresponds to the Faraday geometry when the wave vector \vec{Q} is oriented along the magnetic field direction, $\vec{Q}_{2D} = 0$, and the circular polarizations of light $\vec{\sigma}_{\vec{Q}}^{\pm}$ coincide with the circular polarization vectors of magnetoexciton $\vec{\sigma}_M$, so that $\vec{\sigma}_{\vec{Q}}^+ = \vec{\sigma}_1$ and $\vec{\sigma}_{\vec{Q}}^- = \vec{\sigma}_{-1}$. It means that the light causes the alignment of the magnetoexcitons.²³ At the same time it means the spin polarization of the electron-heavy-hole pair because the magnetoexciton with $M = -1$ is composed of the heavy hole with $j_z = -3/2$ and electron with $s_z = +1/2$, whereas the magnetoexciton with $M = +1$ is composed of the heavy hole with $j_z = 3/2$ and electron with $s_z = -1/2$.

If the optically created electron has the same spin projection as the background electron, then both electrons equally take part in the combined quantum transitions. It results in the enhanced probability of the quantum transition, four times greater than in the case of two electrons with antiparallel spin projections. At the same time it influences the forms of the band shapes giving rise to the contributions of the direct and exchange Coulomb interactions in the case of parallel spin projections or only of the direct Coulomb interaction in the case of antiparallel spin projections. Both these peculiarities are reflected in the formulas for probabilities of the quantum transitions,

$$W(\omega_Q; -; -; \uparrow) = \frac{8\pi v^2}{Ll_0^2} I_l B(\omega_Q) \int_0^\infty x dx e^{-x^2} \times \left[\frac{1}{\pi} + \frac{x^2}{8} \left| {}_1F_1\left(\frac{1}{2}, 2, \frac{x^2}{2}\right) \right|^2 \right] \times \delta \left[\tilde{\Delta} + e^{-x^2/4} I_0\left(\frac{x^2}{4}\right) \right]. \quad (38)$$

Here $x = kl$ and $\tilde{\Delta} = \Delta/I_l$ are the dimensionless wave vector and the energy detuning. The ionization potential of the magnetoexciton $I_{\text{ex}}^{(0,0)}(k)$ was taken in the form

$$I_{\text{ex}}^{(0,0)}(k) = I_l e^{-x^2/4} I_0\left(\frac{x^2}{4}\right), \quad (39)$$

where $I_0(z)$ is the modified Bessel function²⁵ and I_l is the ionization potential at the point $k=0$.

For another circular polarization, in the presence of the same background electrons the probability of combined quantum transition is

$$W(\omega_Q; +; +; \uparrow) = \frac{2\pi v^2}{Ll_0^2} I_l B(\omega_Q) \int_0^\infty x dx e^{-x^2} \delta \left[\tilde{\Delta} + e^{-x^2/4} I_0\left(\frac{x^2}{4}\right) \right]. \quad (40)$$

Integrals (38) and (40) determine the absorption band shapes for two circular polarizations of the light in the Faraday geometry. The probabilities of another two quantum transitions vanish,

$$W(\omega_Q; -; +; \uparrow) = W(\omega_Q; +; -; \uparrow) = 0. \quad (41)$$

If the background electrons are spin polarized in another direction with $s_z = -1/2$, the probabilities of the combined quantum transitions in the Faraday geometry are

$$W(\omega_Q; +; +; \downarrow) = \frac{8\pi v^2}{Ll_0^2} I_l B(\omega_Q) \int_0^\infty x dx e^{-x^2} \times \left[\frac{1}{\pi} + \frac{x^2}{8} \left| {}_1F_1\left(\frac{1}{2}, 2, \frac{x^2}{2}\right) \right|^2 \right] \times \delta \left[\tilde{\Delta} + e^{-x^2/4} I_0\left(\frac{x^2}{4}\right) \right],$$

$$W(\omega_Q; -; -; \downarrow) = \frac{2\pi v^2}{Ll_0^2} I_l B(\omega_Q) \int_0^\infty x dx e^{-x^2} \delta \left[\tilde{\Delta} + e^{-x^2/4} I_0\left(\frac{x^2}{4}\right) \right],$$

$$W(\omega_Q; +; -; \downarrow) = W(\omega_Q; -; +; \downarrow) = 0. \quad (42)$$

The integrals in Eqs. (38), (40), and (42) together with the coefficients $B(\omega_Q)$ determine the band shapes for the whole energy intervals of the absorption bands $-1 \leq \tilde{\Delta} \leq 0$. The analytical expressions of the band shapes can be deduced in the vicinities of the band edges $\tilde{\Delta} \approx 0$ and $\tilde{\Delta} \approx -1$. For example, in the regions $-1 \leq \tilde{\Delta} < -0.9$ and $-0.3 < \tilde{\Delta} \leq 0$ the δ functions select different values of variable x , where the asymptotical expressions of the modified Bessel function as well as of the confluent hypergeometric function do exist. They are

$$e^{-x^2/4} I_0\left(\frac{x^2}{4}\right) = \begin{cases} \left(1 - \frac{x^2}{4}\right), & 0 \leq x < 1 \\ \sqrt{\frac{2}{\pi}} \frac{1}{x}, & 1 < x < \infty, \end{cases}$$

$${}_1F_1\left(\frac{1}{2}; 2; x\right) = \begin{cases} \left(1 + \frac{x}{8}\right), & 0 \leq x < 1 \\ \frac{e^x}{\sqrt{\pi x^{3/2}}}, & 1 < x < \infty. \end{cases} \quad (43)$$

In these two regions the integrals in Eqs. (38) and (40) can be simplified as follows:

$$\begin{aligned}
 f_1(\tilde{\Delta}) &= \int_0^\infty x dx e^{-x^2} \left[\frac{1}{\pi} + \frac{x^2}{8} \left| {}_1F_1\left(\frac{1}{2}, 2, \frac{x^2}{2}\right) \right|^2 \right] \delta\left[\tilde{\Delta} + e^{-x^2/4} I_0\left(\frac{x^2}{4}\right)\right] \\
 &= \begin{cases} \frac{1}{2} \int_0^1 dy e^{-y} \left[\frac{1}{\pi} + \frac{y}{8} \left(1 + \frac{y}{8}\right) \right] \delta\left(\tilde{\Delta} + 1 - \frac{y}{4}\right), & -1 \leq \tilde{\Delta} \leq -0.9 \\ \int_1^\infty x dx e^{-x^2} \left[\frac{1}{\pi} + \frac{e^{x^2}}{\pi x^4} \right] \delta\left(\tilde{\Delta} + \sqrt{\frac{2}{\pi}} \frac{1}{x}\right), & -0.3 \leq \tilde{\Delta} \leq 0. \end{cases} \tag{44}
 \end{aligned}$$

Taking into account that $\delta[f(x)] = \frac{\delta(x-a)}{|f'(x)|_{x=a}}$, we obtained the analytical spectral dependences of the spectral function $f_1(\tilde{\Delta})$,

$$f_1(\tilde{\Delta}) = \begin{cases} e^{-4(1+\tilde{\Delta})} \left[\frac{2}{\pi} + (1+\tilde{\Delta}) + \frac{(1+\tilde{\Delta})^2}{2} \right], & -1 \leq \tilde{\Delta} \leq -0.9 \\ -\frac{2}{\pi^2} \frac{e^{-2/\pi(\tilde{\Delta})^2}}{(\tilde{\Delta})^3} - \frac{\tilde{\Delta}}{2}, & -0.3 \leq \tilde{\Delta} \leq 0. \end{cases} \tag{45}$$

In the case of opposite circular polarization the spectral function $f_2(\tilde{\Delta})$ equals

$$\begin{aligned}
 f_2(\tilde{\Delta}) &= \frac{1}{\pi} \int_0^\infty x dx e^{-x^2} \delta\left[\tilde{\Delta} + e^{-x^2/4} I_0\left(\frac{x^2}{4}\right)\right] \\
 &= \begin{cases} \frac{2}{\pi} e^{-4(1+\tilde{\Delta})}, & -1 \leq \tilde{\Delta} \leq -0.9 \\ -\frac{2}{\pi^2} \frac{e^{-2/\pi(\tilde{\Delta})^2}}{(\tilde{\Delta})^3}, & -0.3 \leq \tilde{\Delta} \leq 0. \end{cases} \tag{46}
 \end{aligned}$$

It can be obtained from expression (45) leaving only the first terms in both limiting cases and removing the second and the third terms.

The spectral functions $f_1(\tilde{\Delta})$ and $f_2(\tilde{\Delta})$ determining the absorption band shapes for two circular polarizations of the light in the Faraday geometry are depicted in Fig. 3. As one can observe both spectral functions $f_1(\tilde{\Delta})$ and $f_2(\tilde{\Delta})$ have the same maximal spectral width equal to 1 in nondimensional energy units, which correspond to ionization potential I_l of magnetoexciton X_{00} at the point $k=0$. It means that all points of the magnetoexciton band take part in the quantum transition due to participation of the background electrons. The maximal width of the band shapes is the same for both circular polarizations because this feature is due exclusively to the momentum conservation law in x in-plane direction in the Landau gauge description. The x components of the wave vectors of the initial photon Q_x , of the magnetoexciton in the final state k_x , of the background electron in the initial state on the LLL with the wave number T , and in the final state on the first-excited LL with the wave number R are all interconnected by the momentum conservation law in this direction,

$$Q_x + T = k_x + R.$$

At a given value of Q_x , a magnetoexciton with arbitrary value of k_x has the possibility to take part in the combined

quantum transitions selecting the needed values T and R of the background electron.

Another feature of the spectral functions is their behavior in the spectral interval $-1 \leq \tilde{\Delta} \leq 0$. The spectral function $f_1(\tilde{\Delta})$ near the point $\tilde{\Delta}=-1$ decreases linearly but with a smaller slope than the function $f_2(\tilde{\Delta})$, which decreases also linearly but faster. In the vicinity of another limiting point $\tilde{\Delta}=0$, the function $f_1(\tilde{\Delta})$ decreases also linearly but faster due exclusively to exchange Coulomb interaction term, while the function $f_2(\tilde{\Delta})$ has a sharp exponentially decrease-

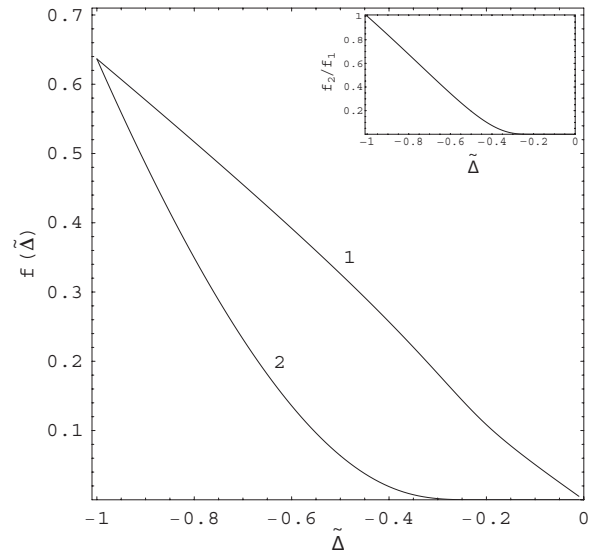


FIG. 3. Spectral functions $f_1(\tilde{\Delta})$ (curve 1) and $f_2(\tilde{\Delta})$ (curve 2) determining the absorption band shapes for two circular polarizations of the light in the Faraday geometry. In the inset the ratio f_2/f_1 in dependence on the $\tilde{\Delta}$.

ing tail. The surface under the curve $f_1(\tilde{\Delta})$ is larger under the curve $f_2(\tilde{\Delta})$.

The final forms of probabilities (38), (40), and (42) for the Faraday geometry are

$$\begin{aligned} W(\omega_Q; \bar{\sigma}_Q^-; -; \uparrow) &= \frac{8\pi v^2}{Ll_0^2} I_l B(\omega_Q) f_1(\tilde{\Delta}), \\ W(\omega_Q; \bar{\sigma}_Q^+; +; \uparrow) &= \frac{2\pi v^2}{Ll_0^2} I_l B(\omega_Q) f_2(\tilde{\Delta}), \\ W(\omega_Q; \bar{\sigma}_Q^+; +; \downarrow) &= \frac{8\pi v^2}{Ll_0^2} I_l B(\omega_Q) f_1(\tilde{\Delta}), \\ W(\omega_Q; \bar{\sigma}_Q^-; -; \downarrow) &= \frac{2\pi v^2}{Ll_0^2} I_l B(\omega_Q) f_2(\tilde{\Delta}), \end{aligned} \quad (47)$$

where the coefficients $B(\omega_Q)$ and the detunings Δ are given by formulas (32) and (23) correspondingly.

The formulas [Eq. (47)] give the full description of the probabilities of the combined quantum transitions and of their band shapes expressed by the products of spectral functions $f_i(\tilde{\Delta})$ and of the coefficients $B(\omega_Q)$, containing resonant denominators in the form

$$B(\omega_Q) \approx \frac{1}{(\Delta + \hbar\omega_{ce})^2} \approx \frac{1}{(\Delta + \hbar\omega_{ce})^2 + \Gamma^2}. \quad (48)$$

Here the damping Γ was introduced phenomenologically. The energy detuning Δ can be changed in the interval $-I_l \leq \Delta \leq 0$ as it is determined by the spectral functions $f_i(\tilde{\Delta})$. As was mentioned in Refs. 21 and 22, the above calculations are true in the range of magnetic field, where the electron cyclotron energy $\hbar\omega_{ce}(H)$ exceeds the value of the ionization potential $I_l(H)$ of magnetoexciton, i.e., in the case $\hbar\omega_{ce}(H) \geq I_l(H)$. For the parameter of GaAs and CdTe crystals it means $H \geq 15-20T$. For these conditions the largest influence of the coefficient $B(\omega_Q)$ on the absorption band shapes is expected in the spectral region $\Delta \cong -I_l$ when $\hbar\omega_{ce} = I_l$ and their sum $(\Delta + \hbar\omega_{ce})$ goes to zero. The calculations were made using the damping $\Gamma = 0.1I_l$, supposing $\hbar\omega_{ce}(H) \geq 2I_l(H)$.

In the above mentioned region the coefficient $B(\omega_Q)$ is proportional to H^{-2} . The factor $v^2 I_l / l_0^2$ can be transcribed as $2\pi n_{el} I_l$, where n_{el} is the concentration of background electrons, $n_{el} = v^2 / 2\pi l_0^2$. The factor $v^2 I_l / l_0^2$ is proportional to $H^{3/2}$ for a given filling factor v^2 or to $H^{1/2}$ for a given electron concentration. Therefore, the probabilities of transition depend on magnetic field as $H^{-1/2}$ for a given filling factor or as $H^{-3/2}$ at given concentration of background electrons.

The probabilities of the quantum transitions with participation of two electrons with parallel spins in their maxima are four times larger than in the case of antiparallel spins. This property was observed experimentally and discussed in Ref. 8. One can see it in Fig. 2b of Ref. 8, where the curves c and d correspond to σ^- and σ^+ polarized excitations. Yakovlev *et al.*⁸ explained the strong circular polarization of the exciton-cyclotron resonance (ExCR) line by the fact that the

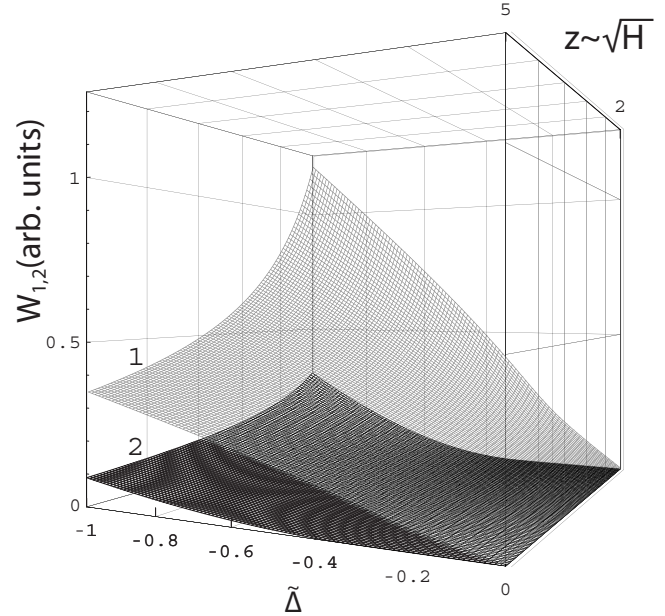


FIG. 4. The absorption band shapes for two circular polarizations in arbitrary units for a given filling factor in dependence on the frequency detuning $\tilde{\Delta}$ and on a parameter $Z = \hbar\omega_{ce}/I_l$ characterizing the magnetic field strength.

new created electron has the same spin orientation as the background electron. This qualitative suggestion coincides with the results of the present paper.

The combined absorption band shapes for two light circular polarizations are depicted in Fig. 4 in arbitrary units for a given filling factor v^2 in dependence on the nondimensional frequency detuning $\tilde{\Delta}$ and on nondimensional parameter characterizing magnetic field strength $z = \hbar\omega_{ce}(H)/I_l(H) \sim \sqrt{H}$. The shifts of two bands due to Zeeman splitting are neglected. The widths of the band shapes are due to inhomogeneous broadening arising from the dispersion law of the magnetoexciton energy band. For the magnetoexciton X_{00} with the electron-hole Landau levels $n_e = n_h = 0$ the maximal width is I_l . The widths of the band shapes 1 and 2 at their half heights in the case $z=2$ equal to $0.51I_l$ and $0.22I_l$ correspondingly. They are much larger than the inhomogeneous broadening of the spectrum introduced by the convolution procedure in Ref. 20 using a Gaussian function of the 0.015 width. The inhomogeneous broadening is determined directly by the Coulomb electron-hole interaction, each of them being in the state of Landau quantization with the distance $\rho = kl_0^2$ between their orbits. Here k is the wave vector of the center-of-mass motion, but we can represent the magnetoexciton energy band as a dependence on ρ . It permits to generalize this result describing the impurity center in a strong magnetic field. For example, in the case of an acceptor center A we can suppose that the hole is in a state of a Landau quantization and the distance between the ion A^- and the hole orbit is R . The mean distance between the hole and the ion A^- will be equal to $\sqrt{l_0^2 + R^2}$ and their Coulomb interaction will be equal to $-e^2/(\epsilon_0\sqrt{l_0^2 + R^2})$. It will generate an energy band in dependence on R of the same type as the exciton energy band in dependence on ρ and k . Here we have

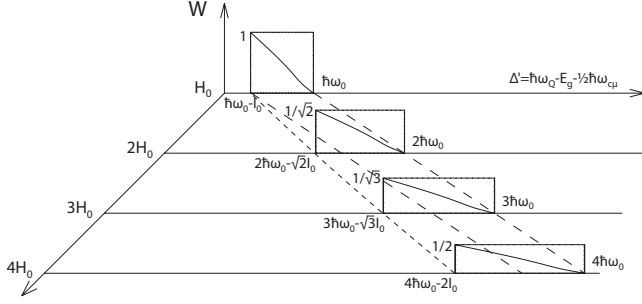


FIG. 5. The absorption band shapes of the combined quantum transitions at a given filling factor and different magnetic field strengths in dependence on the energy detuning $\Delta' = \hbar\omega_Q - E_g - 1/2\hbar\omega_{c\mu}$.

deal with the model of the impurity center in the presence of a high magnetic field or with the model of the magnetoimpurity center similar with the structure of the magnetoexciton. In this model the AX^+ impurity center will give rise to AX^+SU process with the photoluminescence spectrum of the same type as in the case of the combined (ExCR) absorption band shape. The low-energy tail in the AX^+SU process will be of the same type as the high-energy tail in ExCR absorption band. Both of them are due to the inhomogeneous broadening, the origin of which is the Coulomb interaction. In first case it is the Coulomb interaction between the Landau quantized hole and the ion A^- whereas in the second case it is the Coulomb interaction between the Landau quantized electron and hole.

Looking at Fig. 4 one can observe that the both surfaces 1 and 2 are characterized by the decreasing heights when the magnetic field strength increases. At the same time their spectral widths are increased with the increasing magnetic field. It can be observed if one returns to dimensional energy detuning $\Delta = \tilde{\Delta}I_l(H)$, whose maximal absolute value is I_l , and increases as \sqrt{H} with magnetic field strength. This property of the absorption band shape is represented in Fig. 5, where four sections of surface 1 from Fig. 4 are drawn for four multiple values of the magnetic field strength H_0 . We selected some magnetic field strength H_0 and denoted by $\hbar\omega_0 = \hbar\omega_{ce}(H_0)$ the electron cyclotron energy and by I_0 the magnetoexciton ionization potential $I_l(H_0) = I_0$, supposing that $\hbar\omega_0 > I_0$. The magnetic field strength values H being multiple to H_0 are denoted as $H = nH_0$, $n > 1$. The corresponding electron cyclotron energy $\hbar\omega_{ce}(H)$ and ionization potentials $I_l(H)$ can be expressed through $\hbar\omega_0$ and I_0 as follows:

$$\hbar\omega(nH_0) = n\hbar\omega_0, \quad I_l(nH_0) = \sqrt{n}I_0, \quad n > 1.$$

Looking at Fig. 5 one can observe that simultaneously with the decreasing in the absorption band shape heights as $1/\sqrt{H} \approx 1/\sqrt{n}$, the band shape widths are increasing as \sqrt{n} , which results in the conservation of the band shape spectral area at a given filling factor ν^2 . At a given background electron concentration the heights are decreasing as $H^{-3/2}$ whereas the widths are increasing as earlier proportional to \sqrt{H} and the band shape spectral area is decreasing as $1/H$.

The combined magnetoexciton-cyclotron resonance can be described in the first-order perturbation theory if the

quadrupole-active quantum transitions are taken into account.^{8,9,20} The electron-hole pair ($n_e=1$, $s_z=1/2$) and ($n_h=0$, $j_z=-3/2$) can be optically created only in the quadrupole-active quantum transitions. In this case, as was mentioned in Refs. 8 and 9 the optically created hole ($n_h=0$, $j_z=-3/2$) and the resident electron ($n_e=0$, $s_z=1/2$) form the magnetoexciton $X(n_e=n_h=0, M=-1)$, whereas the optically created electron ($n_e=+1$, $s_z=1/2$) is transformed into a background electron on the excited Landau level. Taking this into account and using as earlier the constant approximation for the matrix element P_{cv} we obtain

$$W(\mp; -; \uparrow) = \frac{\pi v^2}{L\omega_Q I_l(H)} \left(\frac{e}{m_0}\right)^2 |P_{cv}|^2 |\vec{Q}_{2D}|^2 \times \exp\left[-\frac{|\vec{Q}_{2D}|^2 l_0^2}{2}\right] |(\vec{\sigma}_{\vec{Q}}^{\mp*} \cdot \vec{\sigma}_{-1})|^2 \times \int_0^\infty x dx \delta\left[\tilde{\Delta} + e^{-x^2/4} I_0\left(\frac{x^2}{4}\right)\right]. \quad (49)$$

It has the same dependence on the magnetic field as in the case of dipole-active transition, but being quadrupole active it is proportional to $|\vec{Q}_{2D}|^2$ and vanishes in Faraday geometry when $\vec{Q}_{2D}=0$. Its angular dependence on the light circular polarization vector is the same as in the dipole-active transitions. The spectral dependence of the band shape at $\tilde{\Delta} \rightarrow -0$ is singularly increasing as $-1/\tilde{\Delta}^3$.

The combined quantum transitions can take place also without cyclotron resonance, i.e., without excitation of the background electron from the lowest to the first-excited Landau level. The resident electrons can accompany the creation of a single magnetoexciton taking part only in the momentum conservation law in the direction of translational symmetry in the Landau gauge description without necessity in supplementary energy for the background electron excitation. The implication of the background electron into the magnetoexciton creation is expressed by the relation $\vec{Q}_x + T = k_x + R$, which permits the exciton with any values k_x to be excited by the photon with wave vector \vec{Q} . Because the quantum numbers of the electron and hole Landau levels equal each other $n_e = n_h = 0$ this optical transition is dipole active, does not vanish in the Faraday geometry, and can be described in the first order of the perturbation theory. The absorption band shape has the same maximal width I_l . It forms a pedestal or a background absorption band proportional to the background electron concentration. The pure magnetoexciton absorption band represents a sharp band because the condition $\vec{k}_{ex} = \vec{Q}_{2D}$ holds, and it is installed over the pedestal in its low energy part.

V. CONCLUSIONS

In the present paper the combined two-dimensional magnetoexciton-cyclotron resonance was described as a dipole-active transition in scope of the second-order perturbation theory in perturbations of the electron-photon interaction and the Coulomb electron-electron interactions. The ma-

trix elements of the electron-photon interaction are proportional to the scalar product of the light and exciton circular polarization vectors ($\vec{\sigma}_Q^{\pm*} \cdot \vec{\sigma}_M$), so that the probability of the optical transition is proportional to $|\langle \vec{\sigma}_Q^{\pm*} \cdot \vec{\sigma}_M \rangle|^2$. The light circular polarization induces optical orientation inside the electron subsystem creating optical alignment of excitons and spin polarization of electrons. Two possible projections of the magnetoexciton orbital momentum on the magnetic field $M = s_z + j_z = \mp 1$ corresponding to the electron-spin projections $s_z = \pm \frac{1}{2}$ and the heavy hole momentum projections $j_z = \mp \frac{3}{2}$ result in the electron-spin polarization. Spin polarization of the optically created electrons is crucial for the ExCR absorption. If the optically created electrons and resident electrons are polarized in the same direction their Coulomb interaction consists of the direct and exchange interaction terms, which results in additional factor 4 in the probability of quantum transition compared to the case of electrons with antiparallel spins, which has been observed experimentally.^{8,9}

The spectral functions $f_i(\Delta)$ in the expression for probabilities have the same maximal heights at the spectral point $\Delta = -I_i$, which corresponds to the bottom of the exciton energy band. However, the width of the spectral functions is different for different circular polarizations due to different contributions of the direct and exchange Coulomb interactions. Also different is the slopes of the spectral functions, though their maximal bandwidth at the bottom is the same and equals the ionization potential I_i of the magnetoexciton. The probability of transition decreases as $1/\sqrt{H}$ with the

magnetic field at a given filling factor and as a $H^{-3/2}$ at a given electron concentration, which can be verified experimentally. The maximum width I_i of the band shape increases as \sqrt{H} , so that the band shape spectral area remains constant at a given filling factor and decreases as $1/H$ for a given electron concentration. This opens additional possibilities for the experimental study of the energy spectrum of the system. In particular, inhomogeneous broadening in the absorption band of ExCR suggests a plausible explanation of the low-energy tail in the photoluminescence band AX⁺SU observed in Ref. 7.

ACKNOWLEDGMENTS

This work was supported by the Grant No. 08.820.05.033RF offered by the Academy of Sciences of Moldova and RFBR as well as by the Grant No. 08.819.05.07F of the Academy of Sciences of Moldova for the young scientists. One of the authors (S.A.M) greatly appreciate support of the Wenner-Gren Foundation during his stay in Uppsala, where the majority of the research has been done.

APPENDIX A: HAMILTONIAN OF THE BAND-TO-BAND OPTICAL TRANSITIONS

The Hamiltonian of electron radiation (1) with the definition of vector potential (2) can be written in the second-quantization representation as follows:

$$\begin{aligned}
\hat{H}_{e\text{-rad}} = & \left(-\frac{e}{m_0} \right) \sum_{\vec{k}(k_x, k_y, k_z)} \sqrt{\frac{2\pi\hbar}{V\omega_k}} \sum_{n_c, n_v} \sum_{g, q} \left\{ \left\{ C_{\vec{k},-}^+ \left[\vec{\sigma}_{\vec{k}}^+ \cdot \vec{\mathcal{P}} \left(\frac{1}{2}, n_c, g; \frac{3}{2}; n_v, q; \vec{k} \right) \right] \right. \right. \\
& + C_{\vec{k},+}^- \left[\vec{\sigma}_{\vec{k}}^- \cdot \vec{\mathcal{P}} \left(\frac{1}{2}, n_c, g; \frac{3}{2}; n_v, q; \vec{k} \right) \right] \left. \right\} a_{1/2, n_c, g}^\dagger a_{3/2, n_v, q} + \left\{ C_{\vec{k},-}^- \left[\vec{\sigma}_{\vec{k}}^- \cdot \vec{\mathcal{P}} \left(-\frac{1}{2}, n_c, g; -\frac{3}{2}; n_v, q; \vec{k} \right) \right] \right. \\
& + C_{\vec{k},+}^+ \left[\vec{\sigma}_{\vec{k}}^+ \cdot \vec{\mathcal{P}} \left(-\frac{1}{2}, n_c, g; -\frac{3}{2}; n_v, q; \vec{k} \right) \right] \left. \right\} a_{-1/2, n_c, g}^\dagger a_{-3/2, n_v, q} + \left\{ C_{\vec{k},-}^+ \left[\vec{\sigma}_{\vec{k}}^+ \cdot \vec{\mathcal{P}} \left(\frac{3}{2}, n_v, q; \frac{1}{2}; n_c, g; \vec{k} \right) \right] \right. \\
& + C_{\vec{k},+}^- \left[\vec{\sigma}_{\vec{k}}^- \cdot \vec{\mathcal{P}} \left(\frac{3}{2}, n_v, q; \frac{1}{2}; n_c, g; \vec{k} \right) \right] \left. \right\} a_{3/2, n_v, q}^\dagger a_{1/2, n_c, g} + \left\{ C_{\vec{k},-}^- \left[\vec{\sigma}_{\vec{k}}^- \cdot \vec{\mathcal{P}} \left(-\frac{3}{2}, n_v, q; -\frac{1}{2}; n_c, g; \vec{k} \right) \right] \right. \\
& + C_{\vec{k},+}^+ \left[\vec{\sigma}_{\vec{k}}^+ \cdot \vec{\mathcal{P}} \left(-\frac{3}{2}, n_v, q; -\frac{1}{2}; n_c, g; \vec{k} \right) \right] \left. \right\} a_{-3/2, n_v, q}^\dagger a_{-1/2, n_c, g} + \left\{ (C_{\vec{k},+}^+)^{\dagger} \left[\vec{\sigma}_{\vec{k}}^+ \cdot \vec{\mathcal{P}} \left(\frac{1}{2}, n_c, g; \frac{3}{2}; n_v, q; -\vec{k} \right) \right] \right. \\
& + (C_{\vec{k},-}^-)^{\dagger} \left[\vec{\sigma}_{\vec{k}}^- \cdot \vec{\mathcal{P}} \left(\frac{1}{2}, n_c, g; \frac{3}{2}; n_v, q; -\vec{k} \right) \right] \left. \right\} a_{1/2, n_c, g}^\dagger a_{3/2, n_v, q} + \left\{ (C_{\vec{k},+}^-)^{\dagger} \left[\vec{\sigma}_{\vec{k}}^- \cdot \vec{\mathcal{P}} \left(-\frac{1}{2}, n_c, g; -\frac{3}{2}; n_v, q; -\vec{k} \right) \right] \right. \\
& + (C_{\vec{k},-}^+)^{\dagger} \left[\vec{\sigma}_{\vec{k}}^+ \cdot \vec{\mathcal{P}} \left(-\frac{1}{2}, n_c, g; -\frac{3}{2}; n_v, q; -\vec{k} \right) \right] \left. \right\} a_{-1/2, n_c, g}^\dagger a_{-3/2, n_v, q} + \left\{ (C_{\vec{k},+}^+)^{\dagger} \left[\vec{\sigma}_{\vec{k}}^+ \cdot \vec{\mathcal{P}} \left(\frac{3}{2}, n_v, q; \frac{1}{2}; n_c, g; -\vec{k} \right) \right] \right. \\
& + (C_{\vec{k},-}^-)^{\dagger} \left[\vec{\sigma}_{\vec{k}}^- \cdot \vec{\mathcal{P}} \left(\frac{3}{2}, n_v, q; \frac{1}{2}; n_c, g; -\vec{k} \right) \right] \left. \right\} a_{3/2, n_v, q}^\dagger a_{1/2, n_c, g} + \left\{ (C_{\vec{k},+}^-)^{\dagger} \left[\vec{\sigma}_{\vec{k}}^- \cdot \vec{\mathcal{P}} \left(-\frac{3}{2}, n_v, q; -\frac{1}{2}; n_c, g; -\vec{k} \right) \right] \right. \\
& + (C_{\vec{k},-}^+)^{\dagger} \left[\vec{\sigma}_{\vec{k}}^+ \cdot \vec{\mathcal{P}} \left(-\frac{3}{2}, n_v, q; -\frac{1}{2}; n_c, g; -\vec{k} \right) \right] \left. \right\} a_{-3/2, n_v, q}^\dagger a_{-1/2, n_c, g}. \tag{A1}
\end{aligned}$$

Using the momentum operator in the form $\hat{P} = \vec{a}_1 \hat{P}_x + \vec{a}_2 \hat{P}_y$ and the hole circular polarization vectors $\vec{\sigma}_M$ [Eq. (5)], we will transform the matrix elements in

$$\begin{aligned}
& \left[\vec{\sigma}_k^\pm \cdot \vec{P} \left(\frac{1}{2}, n_c, g; \frac{3}{2}; n_v, q; \vec{k} \right) \right] \\
&= \int \varphi_{n_c, g}^*(\vec{r}) U_{c, s, g}^*(\vec{r}) e^{i\vec{k}\vec{r}} \\
&\times \frac{1}{\sqrt{2}} [(\vec{\sigma}_k^\pm \cdot \vec{a}_1) \hat{P}_x + (\vec{\sigma}_k^\pm \cdot \vec{a}_2) \hat{P}_y] [U_{v, p, x, q}(\vec{r}) \\
&+ i U_{v, p, y, q}(\vec{r})] \varphi_{n_v, q}(\vec{r}) d\vec{r} = (\vec{\sigma}_k^\pm \cdot \vec{\sigma}_1) \int \varphi_{n_c, g}^*(\vec{r}) U_{c, s, g}^*(\vec{r}) e^{i\vec{k}\vec{r}} \\
&\times \hat{P}_x U_{v, p, x, q}(\vec{r}) \varphi_{n_v, q}(\vec{r}) d\vec{r} = (\vec{\sigma}_k^\pm \cdot \vec{\sigma}_1) A(n_c, g; n_v, q; \vec{k}), \\
& \left[\vec{\sigma}_k^\pm \cdot \vec{P} \left(\frac{3}{2}, n_v, q; \frac{1}{2}; n_c, g; \vec{k} \right) \right] \\
&= \int \varphi_{n_v, q}^*(\vec{r}) [U_{v, p, x, q}^*(\vec{r}) - i U_{v, p, y, q}^*(\vec{r})] e^{i\vec{k}\vec{r}} \\
&\times \frac{1}{\sqrt{2}} [(\vec{\sigma}_k^\pm \cdot \vec{a}_1) \hat{P}_x + (\vec{\sigma}_k^\pm \cdot \vec{a}_2) \hat{P}_y] U_{c, s, g}(\vec{r}) \varphi_{n_c, g}(\vec{r}) d\vec{r} \\
&= (\vec{\sigma}_k^\pm \cdot \vec{\sigma}_{-1}) B(n_v, q; n_c, g; \vec{k}), \tag{A2}
\end{aligned}$$

where

$$\begin{aligned}
& A(n_c, g; n_v, q; \vec{k}) \\
&= \int \varphi_{n_c, g}^*(\vec{r}) U_{c, s, g}^*(\vec{r}) e^{i\vec{k}\vec{r}} \hat{P}_x U_{v, p, x, q}(\vec{r}) \varphi_{n_v, q}(\vec{r}) d\vec{r}, \\
& B(n_v, q; n_c, g; \vec{k}) \\
&= \int \varphi_{n_v, q}^*(\vec{r}) U_{v, p, x, q}^*(\vec{r}) e^{i\vec{k}\vec{r}} \hat{P}_x U_{c, s, g}(\vec{r}) \varphi_{n_c, g}(\vec{r}) d\vec{r}. \tag{A3}
\end{aligned}$$

The coefficients in the expressions [Eq. (A2)] depend on the scalar products of the vectors of circular polarization of the propagating photon $\vec{\sigma}_k^\pm$ and of the valence electrons on the layer $\vec{\sigma}_M$. The wave vector of the propagating photon has an arbitrary direction, whereas $\vec{\sigma}_M$ is oriented along magnetic field direction. In obtaining the expressions [Eq. (A2)] some simplifications were made. It was supposed that

$$\begin{aligned}
& \int \varphi_{n_c, g}^*(\vec{r}) U_{c, s, g}^*(\vec{r}) e^{i\vec{k}\vec{r}} \hat{P}_x U_{v, p, x, q}(\vec{r}) \varphi_{n_v, q}(\vec{r}) d\vec{r} \\
&= \int \varphi_{n_c, g}^*(\vec{r}) U_{c, s, g}^*(\vec{r}) e^{i\vec{k}\vec{r}} \hat{P}_y U_{v, p, y, q}(\vec{r}) \varphi_{n_v, q}(\vec{r}) d\vec{r} \tag{A4}
\end{aligned}$$

and

$$\begin{aligned}
& \int \varphi_{n_c, g}^*(\vec{r}) U_{c, s, g}^*(\vec{r}) e^{i\vec{k}\vec{r}} \hat{P}_x U_{v, p, y, q}(\vec{r}) \varphi_{n_v, q}(\vec{r}) d\vec{r} \\
&= \int \varphi_{n_c, g}^*(\vec{r}) U_{c, s, g}^*(\vec{r}) e^{i\vec{k}\vec{r}} \hat{P}_y U_{v, p, x, q}(\vec{r}) \varphi_{n_v, q}(\vec{r}) d\vec{r} = 0. \tag{A5}
\end{aligned}$$

They are justified by the orthogonality relation of the periodic parts of the Bloch functions when they belong to different bands and are integrated over the volume v_0 of the lattice elementary cell as follows:

$$\begin{aligned}
& \frac{1}{v_0} \int_{v_0} d\vec{\rho} U_{c, s, g}^*(\vec{\rho}) U_{v, p, \xi, q}(\vec{\rho}) = 0, \quad \xi = x, y, \\
& \frac{1}{v_0} \int_{v_0} d\vec{\rho} U_{c, s, g}^*(\vec{\rho}) \frac{\partial}{\partial \rho_y} U_{v, p, x, q}(\vec{\rho}) = 0. \tag{A6}
\end{aligned}$$

Here $v_0 = a_0^3$ and a_0 is the lattice constant.

By definition the matrix element of the band-to-band transition is

$$P_{cv}(\vec{k}, g) = \frac{a_0}{v_0} \int_{v_0} d\vec{\rho} U_{c, s, g}^*(\vec{\rho}) e^{i\vec{k}\vec{\rho}} \left(-i\hbar \frac{\partial}{\partial \rho_x} \right) U_{v, p, x, g-k_x}(\vec{\rho}). \tag{A7}$$

In the case of conduction and valence bands of different parity such matrix element is considered to be of allowed type under the classification of Elliott²⁶ and does not depend on the wave vectors \vec{k} and g . It is true for small deviation of the wave vectors \vec{k} and g from the center of the Brillouin zone. While the light wave vector \vec{k} satisfies to this condition, this dependence must be taken into account for the arbitrary values of g . One possibility is the step function when P_{cv} is a constant in the interval $0 \leq gl_0 \leq 1$ and equals zero at $gl_0 \geq 1$.

For the integration over the volume of the elementary cell v_0 , the coordinate vector \vec{r} is represented as a sum of the 2D vector \vec{R} denoting the 2D lattice points with elementary cell in each site of the monoatomic layer and of a small coordinate vector $\vec{\rho}$ changing inside the volume of the elementary cell as follows:

$$\vec{r} = \vec{R} + \vec{\rho}, \quad \int d\vec{r} = \sum_{\vec{R}} \int_{v_0} d\vec{\rho} = \int_{v_0} d^2\vec{R} \frac{a_0}{v_0} \int_{v_0} d\vec{\rho}. \tag{A8}$$

The periodic parts of the Bloch functions do not depend on \vec{R} because $U_{c, s, g}^*(\vec{R} + \vec{\rho}) = U_{c, s, g}^*(\vec{\rho})$ and $U_{v, p, \xi, q}(\vec{R} + \vec{\rho}) = U_{v, p, \xi, q}(\vec{\rho})$. Since the oscillator-type wave functions of the Landau quantization are localized on the size of the order l_0 much greater than a_0 , their dependences on ρ can be neglected, so that

$$\varphi_{n, q}(R_y + \rho_y) \cong \varphi_{n, q}(R_y). \tag{A9}$$

Small corrections of the order a_0/l_0 were not taken into account.

The dependence of the plane-wave functions on both coordinates \vec{R} and $\vec{\rho}$ is taken into account providing the momentum conservation in x direction. In this way one can integrate separately over v_0 the periodic parts of the Bloch functions keeping their derivatives, so as to avoid their orthogonality. It leads to the integration over the 2D space of the envelope wave functions alone without derivative operator. As a result we obtain

$$\begin{aligned} A(n_c, g; n_v, q; \vec{k}) &= \delta_{kr}(q, g - k_x) \\ &\quad \times \Phi(n_c, g; n_v, g - k_x; k_y) P_{cv}(k_y, g), \\ B(n_v, q; n_c, g; \vec{k}) &= A^*(n_c, g; n_v, q; -\vec{k}) \\ &= \delta_{kr}(q, g + k_x) \Phi^*(n_c, g; n_v, g + k_x; -k_y) \\ &\quad \times P_{cv}^*(-k_y, g). \end{aligned} \quad (\text{A10})$$

The function $\Phi(n_c, g; n_v, q; k_y)$ has the meaning of the normalization and orthogonality integrals, when $\vec{k}=0$, and gives rise to quadrupole corrections proportional to kl_0 when the quantum numbers n_e and n_v differ by unity, $n_e = n_v \pm 1$. They are important in the case of quadrupole-active optical quantum transitions. This function is

$$\begin{aligned} \Phi(n_c, g; n_v, g - k_x; k_y) &= \int dR_y \varphi_{n_c}^*(R_y - gl_0^2) \varphi_{n_v}[R_y - (g - k_x)l_0^2] e^{ik_y R_y} \\ &= e^{ik_y gl_0^2} \int dy \varphi_{n_c}^*(y) \varphi_{n_v}(y + k_x l_0^2) e^{ik_y y}. \end{aligned} \quad (\text{A11})$$

With all these being taken into account, the electron-photon Hamiltonian can be presented in the form

$$\begin{aligned} \hat{H}_{e\text{-rad}} &= \left(-\frac{e}{m_0} \right) \sum_{\vec{k}(k_x, k_y, k_z)} \sqrt{\frac{2\pi\hbar}{V\omega_k}} \sum_{n_c, n_v} \sum_g \{ P_{cv}(k_y, g) \Phi(n_c, g; n_v, g - k_x; k_y) [(C_{\vec{k},-}^-(\vec{\sigma}_{\vec{k}}^+ \cdot \vec{\sigma}_1) + C_{\vec{k},+}^-(\vec{\sigma}_{\vec{k}}^- \cdot \vec{\sigma}_1)) a_{1/2, n_c, g}^\dagger a_{3/2, n_v, g - k_x} \\ &\quad + [C_{\vec{k},-}^-(\vec{\sigma}_{\vec{k}}^+ \cdot \vec{\sigma}_{-1}) + C_{\vec{k},+}^-(\vec{\sigma}_{\vec{k}}^- \cdot \vec{\sigma}_{-1})] a_{-1/2, n_c, g}^\dagger a_{-3/2, n_v, g - k_x} + P_{cv}^*(-k_y, g) \Phi^*(n_c, g; n_v, g + k_x; -k_y) \\ &\quad \times [(C_{\vec{k},-}^-(\vec{\sigma}_{\vec{k}}^+ \cdot \vec{\sigma}_{-1}) + C_{\vec{k},+}^-(\vec{\sigma}_{\vec{k}}^- \cdot \vec{\sigma}_{-1})] a_{3/2, n_v, g + k_x}^\dagger a_{1/2, n_c, g} + [C_{\vec{k},-}^-(\vec{\sigma}_{\vec{k}}^+ \cdot \vec{\sigma}_1) + C_{\vec{k},+}^-(\vec{\sigma}_{\vec{k}}^- \cdot \vec{\sigma}_1)] a_{-3/2, n_v, g + k_x}^\dagger a_{-1/2, n_c, g} \\ &\quad + P_{cv}(-k_y, g) \Phi(n_c, g; n_v, g + k_x; -k_y) [(C_{\vec{k},+}^-(\vec{\sigma}_{\vec{k}}^+ \cdot \vec{\sigma}_1) + (C_{\vec{k},-}^-(\vec{\sigma}_{\vec{k}}^- \cdot \vec{\sigma}_1)) a_{1/2, n_c, g}^\dagger a_{3/2, n_v, g + k_x} + [(C_{\vec{k},+}^-(\vec{\sigma}_{\vec{k}}^+ \cdot \vec{\sigma}_{-1}) \\ &\quad + (C_{\vec{k},-}^-(\vec{\sigma}_{\vec{k}}^- \cdot \vec{\sigma}_{-1})] a_{-1/2, n_c, g}^\dagger a_{-3/2, n_v, g + k_x} + P_{cv}^*(k_y, g) \Phi^*(n_c, g; n_v, g - k_x; k_y) [(C_{\vec{k},+}^-(\vec{\sigma}_{\vec{k}}^+ \cdot \vec{\sigma}_{-1}) \\ &\quad + (C_{\vec{k},-}^-(\vec{\sigma}_{\vec{k}}^- \cdot \vec{\sigma}_{-1})] a_{3/2, n_v, g - k_x}^\dagger a_{1/2, n_c, g} + [(C_{\vec{k},+}^-(\vec{\sigma}_{\vec{k}}^+ \cdot \vec{\sigma}_1) + (C_{\vec{k},-}^-(\vec{\sigma}_{\vec{k}}^- \cdot \vec{\sigma}_1)) a_{-3/2, n_v, g - k_x}^\dagger a_{-1/2, n_c, g}] \}. \end{aligned} \quad (\text{A12})$$

APPENDIX B: SECOND-ORDER MATRIX ELEMENTS

The second-order matrix elements $Z(i|F)$ are calculated using a general formula,

$$Z(i|F) = \sum_u \frac{\langle i | H_{er} | u \rangle \langle u | H_C | F \rangle}{E_i - E_u}. \quad (\text{B1})$$

It has the following concrete realizations:

$$\begin{aligned} Z(i, \mp, \uparrow | F, -, \uparrow) &= \sum_{|u, -, \uparrow\rangle} \frac{\langle i, \mp, \uparrow | \hat{H}_{er} | u, -, \uparrow \rangle \langle u, -, \uparrow | \hat{H}_C | F, -, \uparrow \rangle}{E_{i, \uparrow} - E_{u, -, \uparrow}} = (\vec{\sigma}_{\vec{Q}}^\pm \cdot \vec{\sigma}_{-1}) Z(-, \vec{k}_{\text{ex}} - \vec{Q}_{2D}, \uparrow, T, R), \\ Z(i, \mp, \uparrow | F, +, \uparrow) &= \sum_{|u, +, \uparrow\rangle} \frac{\langle i, \mp, \uparrow | \hat{H}_{er} | u, +, \uparrow \rangle \langle u, +, \uparrow | \hat{H}_C | F, +, \uparrow \rangle}{E_{i, \uparrow} - E_{u, +, \uparrow}} = (\vec{\sigma}_{\vec{Q}}^\pm \cdot \vec{\sigma}_1) Z(+, \vec{k}_{\text{ex}} - \vec{Q}_{2D}, \uparrow, T, R). \end{aligned} \quad (\text{B2})$$

Here $Z(\pm, \vec{k}_{\text{ex}} - \vec{Q}_{2D}, \uparrow, T, R)$ denoted the following expressions:

$$\begin{aligned}
Z(-, \vec{k}_{\text{ex}} - \vec{Q}_{2\text{D}}, \uparrow, T, R) &= 2 \left(-\frac{e}{m_0} \right) \frac{e^{ik_y(k_x/2 - Q_x)l_0^2}}{\sqrt{N}} \sqrt{\frac{2\pi\hbar}{V\omega_Q}} \frac{\delta_{kr}(Q_x + T, k_x + R)}{[\hbar\omega_Q - E_g - \frac{1}{2}\hbar\omega_{c\mu} - (\frac{3}{2}g_h - \frac{1}{2}g_e)\mu_B H]} \sum_f P_{cv}^*(Q_y, f) e^{ik_y f l_0^2} \\
&\quad \times \Phi^*(0, f; 0, f - Q_x; Q_y) [F_{e-e}(0, k_x - Q_x + R; 0, f; 1, R; 0, k_x - Q_x + f) \\
&\quad - F_{e-e}(0, f; 0, k_x - Q_x + R; 1, R; 0, k_x - Q_x + f)] \quad (\text{B3})
\end{aligned}$$

and

$$\begin{aligned}
Z(+, \vec{k}_{\text{ex}} - \vec{Q}_{2\text{D}}, \uparrow, T, R) &= \left(-\frac{e}{m_0} \right) \frac{e^{ik_y(k_x/2 - Q_x)l_0^2}}{\sqrt{N}} \sqrt{\frac{2\pi\hbar}{V\omega_Q}} \frac{\delta_{kr}(Q_x + T, k_x + R)}{[\hbar\omega_Q - E_g - \frac{1}{2}\hbar\omega_{c\mu} + (\frac{3}{2}g_h - \frac{1}{2}g_e)\mu_B H]} \sum_f P_{cv}^*(Q_y, f) e^{ik_y f l_0^2} \\
&\quad \times \Phi^*(0, f; 0, f - Q_x; Q_y) F_{e-e}(0, f; 0, k_x - Q_x + R; 0, k_x - Q_x + f; 1, R). \quad (\text{B4})
\end{aligned}$$

Another second-order matrix elements are

$$\begin{aligned}
Z(i, \mp, \downarrow | F, -, \downarrow) &= \sum_{|u, -, \downarrow} \frac{\langle i, \mp, \downarrow | \hat{H}_{e\text{-rad}} | u, -, \downarrow \rangle \langle u, -, \downarrow | \hat{H}_C | F, -, \downarrow \rangle}{(E_{i\downarrow} - E_{u, -, \downarrow})} \\
&= (\vec{\sigma}_Q^\pm \cdot \vec{\sigma}_{-1}) Z(-, \vec{k}_{\text{ex}} - \vec{Q}_{2\text{D}}, \downarrow, T, R), \\
Z(i, \mp, \downarrow | F, +, \downarrow) &= \sum_{|u, +, \downarrow} \frac{\langle i, \mp, \downarrow | \hat{H}_{e\text{-rad}} | u, +, \downarrow \rangle \langle u, +, \downarrow | \hat{H}_C | F, +, \downarrow \rangle}{(E_{i\downarrow} - E_{u, +, \downarrow})} \\
&= (\vec{\sigma}_Q^\pm \cdot \vec{\sigma}_1) Z(+, \vec{k}_{\text{ex}} - \vec{Q}_{2\text{D}}, \downarrow, T, R). \quad (\text{B5})
\end{aligned}$$

The coefficient $Z(-, \vec{k}_{\text{ex}} - \vec{Q}_{2\text{D}}, \downarrow, T, R)$ describes the case when optically created electron has an opposite spin projection with regard to the background electron; it contains the contribution of the direct Coulomb interaction and has the denominator determined by the difference $(E_{i\downarrow} - E_{u, -, \downarrow})$. It is similar to the coefficient $Z(+, \vec{k}_{\text{ex}} - \vec{Q}_{2\text{D}}, \uparrow, T, R)$ because in this case the optically created electron has a spin projection $s_z = -\frac{1}{2}$, which is antiparallel to the spin projection of the background electron $s_z = \frac{1}{2}$. The last coefficient also depends only on the direct Coulomb interaction. Its denominator coincides with the previous case when the Zeeman splitting is neglected. In the same way the coefficients $Z(+, \vec{k}_{\text{ex}} - \vec{Q}_{2\text{D}}, \downarrow, T, R)$ from Eq. (B5) and $Z(-, \vec{k}_{\text{ex}} - \vec{Q}_{2\text{D}}, \uparrow, T, R)$ from formula (B3) reflect the situations with two parallel electron spins. In the former case they both correspond to $s_z = -\frac{1}{2}$; in the latter case they are equal to $s_z = \frac{1}{2}$. As a result both coefficients depend on the Coulomb direct and exchange interactions. These two coefficients equal exactly each other when the Zeeman splitting is neglected.

As was mentioned in Appendix A the matrix element $P_{cv}(Q_y, f)$ depends on f . When its value changes in the whole Brillouin zone, the constant approximation for $P_{cv}(Q_x, f)$ proposed by Elliott²⁶ in the case of the allowed band-to-band quantum transitions can be insufficient. Nevertheless we will use it because the Coulomb matrix elements taking part in the summation on f are quickly decreasing functions of f .

Using property (A11) of the integral $\Phi(0, f; 0, f - Q_x; Q_y) = e^{ifQ_y l_0^2} \Phi(0, 0; 0, -Q_x; Q_y)$ and neglecting the difference of $\Phi(0, 0; 0, -Q_x; Q_y)$ from unity we simplified the sums on f in formulas (B3) and (B4) as follows:

$$\begin{aligned}
&\sum_f P_{cv}^*(Q_y, f) \Phi^*(0, f; 0, f - Q_x; Q_y) e^{ik_y f l_0^2} \\
&\quad \times [F_{e-e}(0, k_x - Q_x + f; 0, f; 1, R; 0, k_x - Q_x + f) \\
&\quad - F_{e-e}(0, f; 0, k_x - Q_x + R; 1, R; 0, k_x - Q_x + f)] \\
&\quad \equiv P_{cv}^* \sum_f e^{i(k_y - Q_y) f l_0^2} \\
&\quad \times [F_{e-e}(0, k_x - Q_x + R; 0, f; 1, R; 0, k_x - Q_x + f) \\
&\quad - F_{e-e}(0, f; 0, k_x - Q_x + R; 1, R; 0, k_x - Q_x + f)] \\
&\quad = P_{cv}^* [H(\vec{k}_{\text{ex}} - \vec{Q}_{2\text{D}}; R) - F(\vec{k}_{\text{ex}} - \vec{Q}_{2\text{D}}; R)], \quad (\text{B6})
\end{aligned}$$

where

$$\begin{aligned}
H(\vec{k}_{\text{ex}} - \vec{Q}_{2\text{D}}; R) &= \sum_f e^{i(k_y - Q_y) f l_0^2} F_{e-e} \\
&\quad \times (0, k_x - Q_x + R; 0, f; 1, R; 0, k_x - Q_x + f) \\
&= e^{i(k_y - Q_y) R l_0^2} H(\vec{k}_{\text{ex}} - \vec{Q}_{2\text{D}}) F(\vec{k}_{\text{ex}} - \vec{Q}_{2\text{D}}; R) \\
&= \sum_f e^{i(k_y - Q_y) f l_0^2} F_{e-e}(0, f; 0, k_x - Q_x \\
&\quad + R; 1, R; 0, k_x - Q_x + f) \\
&= e^{i(k_y - Q_y) R l_0^2} F(\vec{k}_{\text{ex}} - \vec{Q}_{2\text{D}}). \quad (\text{B7})
\end{aligned}$$

The last functions $H(\vec{k}_{\text{ex}} - \vec{Q}_{2\text{D}})$ and $F(\vec{k}_{\text{ex}} - \vec{Q}_{2\text{D}})$ are derived below. The $\vec{Q}_{2\text{D}}$ vector is the projection of the 3D wave vector \vec{Q} on the plane of the layer.

The direct Coulomb interaction in the first sum [Eq. (B7)] and the exchange Coulomb interaction in the second sum [Eq. (B7)] are derived in Refs. 21 and 22 and have the form

$$\begin{aligned}
F_{e-e}(0, p; 0, q; 1, p - s; 0, q + s) \\
= \sum_{\kappa} W_{s, \kappa} \exp[i\kappa(p - q - s)l_0^2] \frac{(s + i\kappa)l_0}{\sqrt{2}}, \quad (\text{B8})
\end{aligned}$$

where

$$W_{s,\kappa} = V_{s,\kappa} \exp\left[-\frac{(s^2 + \kappa^2)l_0^2}{2}\right],$$

$$V_{s,\kappa} = \frac{2\pi e^2}{\varepsilon_0 S \sqrt{s^2 + \kappa^2}}, \quad (\text{B9})$$

and ε_0 is the background dielectric constant. Taking into account that

$$\sum_f \exp[if(k_y - Q_y - \kappa)] = N \delta_{kr}(\kappa, k_y - Q_y), \quad (\text{B10})$$

we obtain

$$H(\vec{k} - \vec{Q}_{2D}, R) = e^{i(k_y - Q_y)Rl_0^2} H(\vec{k} - \vec{Q}_{2D}), \quad (\text{B11})$$

where

$$H(\vec{k} - \vec{Q}_{2D}) = I_l \exp\left[-\frac{|\vec{k} - \vec{Q}_{2D}|^2 l_0^2}{2}\right] \times \frac{[(k_x - Q_x) + i(k_y - Q_y)]l_0}{\sqrt{\pi}|\vec{k} - \vec{Q}_{2D}|l_0}. \quad (\text{B12})$$

Here I_l is the ionization potential of the magnetoexciton with wave vector $\vec{k}=0$; $I_l = \frac{e^2}{\varepsilon_0 l_0} \sqrt{\frac{\pi}{2}}$.

The calculation of the expression $F(\vec{k} - \vec{Q}_{2D})$ leads to the sum

$$F(\vec{k} - \vec{Q}_{2D}) = \sum_{t,\kappa} W_{t,\kappa} \exp\{i[(k_y - Q_y)t - \kappa(k_x - Q_x)]l_0^2\} \times \frac{(t + i\kappa)l_0}{\sqrt{2}} = \sum_{\vec{P}} W_{\vec{P}} \exp\left\{i \frac{[\vec{P} \times (\vec{k} - \vec{Q}_{2D})]_z l_0^2}{2}\right\} \frac{(P_x + iP_y)l_0}{\sqrt{2}}. \quad (\text{B13})$$

Using the series expansion on the Bessel function,²⁷

$$e^{iz \sin \varphi} = J_0(z) + 2 \sum_{k=1}^{\infty} J_{2k}(z) \cos(2k\varphi) + 2i \sum_{k=0}^{\infty} J_{2k+1}(z) \sin[(2k+1)\varphi],$$

we obtained

$$F(\vec{k} - \vec{Q}_{2D}) = -I_l \frac{|\vec{k} - \vec{Q}_{2D}|l_0}{2\sqrt{2}} \exp\left[-\frac{|\vec{k} - \vec{Q}_{2D}|^2 l_0^2}{2}\right] \times {}_1F_1\left(\frac{1}{2}, 2, \frac{|\vec{k} - \vec{Q}_{2D}|^2 l_0^2}{2}\right), \quad (\text{B14})$$

where ${}_1F_1(a, b, x)$ is the confluent hypergeometric function.²⁵ The square of the absolute values of the functions $H(\vec{k} - \vec{Q}_{2D})$ and $H(\vec{k} - \vec{Q}_{2D}) - F(\vec{k} - \vec{Q}_{2D})$ are

$$|H(\vec{k} - \vec{Q}_{2D})|^2 = \frac{I_l^2}{\pi} \exp[-|\vec{k} - \vec{Q}_{2D}|^2 l_0^2], \quad (\text{B15})$$

$$|H(\vec{k} - \vec{Q}_{2D}) - F(\vec{k} - \vec{Q}_{2D})|^2 = I_l^2 \exp[-|\vec{k} - \vec{Q}_{2D}|^2 l_0^2] \times \left\{ \frac{1}{\pi} + \frac{|\vec{k} - \vec{Q}_{2D}|^2 l_0^2}{8} \left| {}_1F_1\left(\frac{1}{2}, 2, \frac{|\vec{k} - \vec{Q}_{2D}|^2 l_0^2}{2}\right) \right|^2 + \frac{(k_x - Q_x)l_0}{\sqrt{2\pi}} {}_1F_1\left(\frac{1}{2}, 2, \frac{|\vec{k} - \vec{Q}_{2D}|^2 l_0^2}{2}\right) \right\}.$$

They will be used for the calculation of the probabilities of the quantum transitions and of the absorption band shapes.

*exciton@phys.asm.md

¹L. V. Butov, V. I. Grinev, V. D. Kulakovskii, and T. G. Anderson, Phys. Rev. B **46**, 13627 (1992).

²K. J. Nash, M. S. Skolnick, M. K. Saker, and S. J. Bass, Phys. Rev. Lett. **70**, 3115 (1993).

³M. S. Skolnick, K. J. Nash, M. K. Saker, and S. J. Bass, Phys. Rev. B **50**, 11771 (1994).

⁴I. Bar-Joseph, Semicond. Sci. Technol. **20**, R29 (2005).

⁵G. Finkelstein, H. Shtrikman, and I. Bar-Joseph, Phys. Rev. B **56**, 10326 (1997).

⁶G. Finkelstein, H. Shtrikman, and I. Bar-Joseph, Phys. Rev. B **53**, R1709 (1996).

⁷L. Bryja, A. Wojs, J. Misiewicz, M. Potemski, D. Reuter, and A. Wieck, Phys. Rev. B **75**, 035308 (2007).

⁸D. R. Yakovlev, V. P. Kochereshko, R. A. Suris, H. Schenk, W.

Ossau, A. Waag, G. Landwehr, P. C. M. Christianen, and J. C. Maan, Phys. Rev. Lett. **79**, 3974 (1997).

⁹V. P. Kochereshko, D. R. Yakovlev, R. A. Suris, G. V. Astakhov, W. Faschinger, W. Ossau, G. Landwehr, T. Wojtowicz, G. Karczewski, and J. Kossut, *Optical Properties of 2D Systems with Interacting Electrons*, NATO Advanced Studies Institute, (2002), p. 125.

¹⁰G. V. Astakhov, D. R. Yakovlev, V. P. Kochereshko, W. Ossau, J. Nurnberger, W. Faschinger, and G. Landwehr, Phys. Rev. B **60**, R8485 (1999).

¹¹C. Kallin and B. I. Halperin, Phys. Rev. B **30**, 5655 (1984).

¹²A. Wójs, A. Gladysiewicz, and J. J. Quinn, Phys. Rev. B **73**, 235338 (2006).

¹³A. B. Dzyubenko, Phys. Rev. B **65**, 035318 (2001).

¹⁴A. B. Dzyubenko and A. Yu. Sivachenko, Phys. Rev. Lett. **84**,

- 4429 (2000).
- ¹⁵A. Wójs and J. J. Quinn, Phys. Rev. B **63**, 045303 (2000).
- ¹⁶V. M. Apalkov and E. I. Rashba, Phys. Rev. B **46**, 1628 (1992).
- ¹⁷E. I. Rashba and M. E. Portnoi, Phys. Rev. Lett. **70**, 3315 (1993).
- ¹⁸A. Wójs, J. J. Quinn, and P. Hawrylak, Phys. Rev. B **62**, 4630 (2000).
- ¹⁹A. H. MacDonald, E. H. Rezayi, and D. Keller, Phys. Rev. Lett. **68**, 1939 (1992).
- ²⁰A. B. Dzyubenko, Phys. Rev. B **64**, 241101(R) (2001).
- ²¹S. A. Moskalenko, M. A. Liberman, P. I. Khadzhi, E. V. Dumanov, I. V. Podlesny, and V. V. Bořan, Physica E (Amsterdam) **39**, 137 (2007).
- ²²S. A. Moskalenko, M. A. Liberman, P. I. Khadzhi, E. V. Dumanov, I. V. Podlesny, and V. Bořan, Solid State Commun. **140**, 236 (2006).
- ²³*Modern Problems in Condensed-Matter Sciences*, edited by V. M. Agranovich and A. A. Maradudin (North-Holland, Amsterdam, 1984); *Optical Orientation*, edited by F. Meier and B. P. Zakharchenya, Vol. 8.
- ²⁴L. P. Gor'kov and I. E. Dzyaloshinskii, Zh. Eksp. Teor. Fiz. **53**, 717 (1967) [Sov. Phys. JETP **26**, 449 (1968)].
- ²⁵I. S. Gradshteyn and I. M. Ryzhik, *Tables of Integrals, Sums, Series and Products* (Academic, New York, 1965).
- ²⁶R. J. Elliott, Phys. Rev. **108**, 1384 (1957).
- ²⁷G. Korn and T. Korn, *Mathematical Handbook for Scientists and Engineers* (Nauka, Moscow, 1968).